

# ECOGRAPHY

## Improving estimates of species distribution change by incorporating local trends

Journal:	<i>Ecography</i>
Manuscript ID	ECOG-05176.R1
Wiley - Manuscript type:	Research
Keywords:	spatiotemporal modeling, monitoring, species distribution modeling, spatial management
Abstract:	<p>Species distribution models and environmental niche models have evolved rapidly over the last decade to better understand how species' distributions change over space and time. A limitation of conventional metrics (e.g., center of gravity) to assess changes in distribution is that changes may not be spatially heterogeneous. We develop a modeling approach to estimate a spatially explicit temporal trend (i.e., local trend), alongside spatial (temporally constant) and spatiotemporal (time-varying) components, to compare inferred spatial shifts to those indicated by conventional metrics. To demonstrate the utility of this new approach, we focus on the application of this model to a community of well-studied marine fish species on the US west coast (19 species, representing a wide range of presence-absence and densities). Results from conventional model selection indicate that the use of the model accounting for local trends is clearly justified for 89% of these species. In addition to making more parsimonious and accurate predictions, we illustrate how estimated spatial fields from the local trend model can be used to classify regions within the species range where change is relatively heterogeneous or homogenous. Conventional summary metrics, such as center of gravity, can then be calculated on each such region or within previously defined biogeographic boundaries. We use this approach to illustrate that change is more nuanced than what is expressed via global metrics. Using arrowtooth flounder (<i>Atheresthes stomias</i>) as an example, the observed southward shift over time in the global center of gravity is not reflective of a uniform shift in densities but local trends of decreasing density in the northern region and rapidly increasing density at the southern edge of the species' range. Thus, estimating local trends with spatiotemporal models improves interpretation of species distribution change.</p>

1    **Improving estimates of species distribution change by incorporating local trends**

For Review Only

## 2 Abstract

3 Species distribution models and environmental niche models have evolved rapidly over the last  
4 decade to better understand how species' distributions change over space and time. A limitation  
5 of conventional metrics (e.g., center of gravity) to assess changes in distribution is that changes  
6 may not be spatially heterogeneous. We develop a modeling approach to estimate a spatially  
7 explicit temporal trend (i.e., local trend), alongside spatial (temporally constant) and  
8 spatiotemporal (time-varying) components, to compare inferred spatial shifts to those indicated  
9 by conventional metrics. To demonstrate the utility of this new approach, we focus on the  
10 application of this model to a community of well-studied marine fish species on the US west  
11 coast (19 species, representing a wide range of presence-absence and densities). Results from  
12 conventional model selection indicate that the use of the model accounting for local trends is  
13 clearly justified for 89% of these species. In addition to making more parsimonious and accurate  
14 predictions, we illustrate how estimated spatial fields from the local trend model can be used to  
15 classify regions within the species range where change is relatively heterogeneous or  
16 homogenous. Conventional summary metrics, such as center of gravity, can then be calculated  
17 on each such region or within previously defined biogeographic boundaries. We use this  
18 approach to illustrate that change is more nuanced than what is expressed via global metrics.  
19 Using arrowtooth flounder (*Atheresthes stomias*) as an example, the observed southward shift  
20 over time in the global center of gravity is not reflective of a uniform shift in densities but local  
21 trends of decreasing density in the northern region and rapidly increasing density at the southern  
22 edge of the species' range. Thus, estimating local trends with spatiotemporal models improves  
23 interpretation of species distribution change.

24    **Keywords:** spatiotemporal modeling, species distribution modeling, spatial management,  
25    monitoring

For Review Only

## 26    **Introduction**

27    In the fields of natural resource conservation, management, and global change biology, demand  
28    for and implementation of tools for assessing species distribution shifts has grown dramatically  
29    in recent decades (Elith and Leathwick 2009). These approaches are widely applicable, from  
30    studies of plants (Lenoir et al. 2008), terrestrial vertebrates (Hitch and Leberg 2007), and marine  
31    fishes (Pinsky et al. 2013). However, the way distribution shifts are quantified has changed  
32    relatively little (Elith et al. 2010). At the simplest level, researchers often use existing tools to  
33    estimate occurrence probability, present maps of how the extent and distribution of suitable  
34    habitat is expected to change, and sometimes present descriptive statistics on the mean change  
35    throughout a region (Yackulic et al. 2013). Yet, when reliable abundance data are available,  
36    distribution shifts are more robustly quantified by spatial predictions of population size because  
37    these are a richer form of data that are less sensitive to detection issues and anomalous  
38    observations of single individuals (e.g., Tingley and Beissinger 2009), while being more likely to  
39    detect persistent distribution shifts caused by more nuanced factors than absolute physiological  
40    limits. For example, while much species distribution modeling focuses on how drivers such as  
41    climate change may predict change in species' range limits, the core of a species' distribution  
42    may shift due to the influence of multiple drivers on the geography of abundance via movement,  
43    dispersal, and heterogeneity in demographic rates (e.g., age- or size-specific fecundity, somatic  
44    growth, and mortality; Sagarin et al. 2006). Shifting distributions of abundance or population  
45    density may also be qualitatively conveyed through maps, but quantitative spatial indicators can  
46    also be provided, such as the mean location weighted by population density (also termed the  
47    "center of gravity", COG).

48            Spatial distributions of population density are often complex and heterogeneous (Sagarin  
49 and Gaines 2002, Sagarin et al. 2006). Heterogeneity may be present in the distribution of a  
50 species throughout its range, but the change in a species' population density over time may also  
51 have a spatially varying component. Mechanisms responsible for spatial variability in change  
52 might be biological (e.g., variation in birth and death rates) or forced by spatially structured  
53 pressures (such as environmental or habitat change, and anthropogenic disturbances, e.g., Barnett  
54 et al. 2019 and references therein). Consequently, attempting to describe a uniform shift in  
55 distribution across a broad geographic range can be misleading (Sagarin et al. 2006), particularly  
56 when different regions exhibit contrasting trends. For example, if densities increase at opposing  
57 range boundaries at an equivalent rate, there may be no trend in the range-wide COG, masking  
58 finer-scale shifts. Thus, when using spatial indicators to describe species distribution shifts, the  
59 spatial scale of aggregation can affect inference (e.g., Connor et al. 2019), as in the classic  
60 problem of pattern and scale in ecology (Levin 1992). Therefore, there is a general need to  
61 develop objective methods for defining appropriate scales to evaluate changes in species  
62 distributions. Such tools are widely applicable for solving specific problems in fish and wildlife  
63 conservation and management by defining spatial domains with distinct population trends.

64            Techniques for estimating how populations vary over space and time evolved rapidly  
65 with increases in computational power and the development of novel methods and applications  
66 of tools such as hierarchical statistical models. Some of the largest methodological changes have  
67 been advances in spatiotemporal analyses that model space continuously and explicitly  
68 accounted for spatial autocorrelation between spatially referenced observations that are  
69 proximate in both space and time (e.g., Banerjee et al. 2008, Finley et al. 2009, Latimer et al.  
70 2009, Cressie and Wikle 2011, Shelton et al. 2014, Thorson et al. 2015). There are a number of

71 advantages of estimating a species' density in a framework that accounts for spatial or  
72 spatiotemporal variation. First, explicitly accounting for spatial variation in density has been  
73 shown to increase precision of estimated temporal trends (Thorson et al. 2015). Second,  
74 modeling spatial or spatiotemporal variation in population density can be performed within  
75 flexible and established frameworks such as mixed-effect models where the spatial or  
76 spatiotemporal components are estimated as random effects (e.g., Latimer et al. 2009, Cressie  
77 and Wikle 2011, Shelton et al. 2014). Similar to their non-spatial predecessors, these  
78 spatiotemporal modeling approaches often treat time as a discrete factor to allow for unbiased  
79 estimates of temporal trends. With such approaches, the spatial distribution of density can either  
80 be constant (modeled as a single spatial field) or time-varying (with variability modeled either as  
81 independent over time, or as an autoregressive process).

82 These, and similar spatial model-based estimators, have in many applications replaced  
83 conventional design-based estimators of population density, which assume that density is  
84 homogenous within sampling strata (Chen et al. 2004). In addition to being used for estimating  
85 population density or spatial distributions, output from these modeling approaches has been used  
86 to generate model-based summaries to track change in species distributions, including the COG  
87 or area occupied, with more robust estimation than those provided by design-based estimates  
88 (Thorson et al. 2016a). As tools to implement these methods have become accessible in open  
89 source software, such as INLA (Rue et al. 2009), VAST (Thorson 2019b), or sdmTMB  
90 (Anderson et al. 2019, 2020), these approaches have seen broad application to populations in  
91 diverse ecosystems around the world, including terrestrial plants (Banerjee et al. 2008, Finley et  
92 al. 2009, Latimer et al. 2009) and animals (e.g., Thorson et al. 2016b), freshwater (Hocking et al.

93 2018) and marine communities (Shelton et al. 2014, Thorson et al. 2015, 2016a, Thorson and  
94 Barnett 2017, Anderson and Ward 2019).

95 Spatiotemporal modeling of population density has particularly flourished in the field of  
96 marine fisheries, where practical constraints limit the use of spatial capture-recapture, distance  
97 sampling, and other survey methods typically applied in terrestrial and freshwater systems that  
98 have led to parallel development of models for similar purposes (Efford 2004, 2011, Royle and  
99 Young 2008, Royle et al. 2013). The most reliable estimates of marine fish densities at broad  
100 scales are generally derived from fishery-independent surveys where observations of population  
101 density are taken to be proportional to the catch-per-unit-effort of a fishing gear, often  
102 implemented using some form of stratified random sampling design. In addition to providing the  
103 data on population size and structure that is needed for managing individual fish populations,  
104 fishery-independent survey data are used for purposes such as informing ecosystem-based  
105 management (Link et al. 2002, Nicholson and Jennings 2004, Harvey et al. 2018), evaluating the  
106 impacts of harvesting non-target species (Stock et al. 2019), and quantifying shifts in species  
107 distributions (Pinsky et al. 2013, Thorson et al. 2016a). Changes in the spatial distribution of  
108 marine fishes have significant implications for community structure and national food security  
109 (Rice and Garcia 2011). Thus, robust predictions of marine fish distribution shifts are needed, yet  
110 difficult to obtain given sparse and often uneven sampling effort, short monitoring time series,  
111 limited ability to repeat-sample individuals, and the complexities of surveying open populations  
112 with rich spatial structure. Spatial heterogeneity is particularly strong in these marine  
113 ecosystems, where complex coastline and bathymetric topography and geology interact with  
114 physical oceanographic drivers (Levin et al. 2010). Therefore, it is critical to determine to what

115 degree such heterogeneity must be accounted for to adequately characterize marine fish  
116 distribution shifts.

117 Here, we introduce a new approach to address how estimates of change in species  
118 distributions are dependent on the spatial scale of quantitative indicators of species distribution.  
119 We describe the development of a modeling technique that explicitly accounts for spatial  
120 variability in how population densities change through time to estimate finer-scale indicators of  
121 species distribution shifts (local trends). While widely applicable to a wide range of biological  
122 data (or even non-biological data), we focus on an application to changes in the distribution of  
123 commercially fished marine species. These represent 19 species from a 15-year publicly  
124 available trawl survey dataset. We illustrate how our new approach may be used to infer changes  
125 over time, and also how output from this modeling approach may be useful in identifying spatial  
126 regions where change is greater or lesser than average. Specifically, we compare interpretations  
127 of species distribution shifts along a spectrum of indicators from coarse-scales (global COG  
128 trends calculated over an entire survey domain), to moderate- (regional COG trends) and fine-  
129 scales (local trend).

130

## 131 **Material and methods**

### 132 *Spatial GLMM overview*

133 The majority of recent applications of species distribution models (SDMs) to marine fish survey  
134 data have been implemented in a GLMM (generalized linear mixed-effects model) framework,  
135 where random effects are used to describe spatial or spatiotemporal components. Spatial  
136 components are differentiated from spatiotemporal components in that the former are constant,

137 whereas the latter vary through time. Examples include applications to Gaussian predictive  
138 process models (e.g., Shelton et al. 2014, Anderson and Ward 2019), and predictive modeling  
139 using integrated nested Laplace approximations (INLA; e.g., Rue et al. 2009, Ruiz-Cárdenas et  
140 al. 2012, Thorson et al. 2015). The latter approach has been particularly useful for large datasets,  
141 where substantial gains in computational efficiency are accomplished by taking advantage of  
142 sparse matrix approximations to the variance-covariance matrix (Thorson and Barnett 2017).  
143 Regardless of the estimation approach used, the general formulation of these models uses a link  
144 function  $g(\cdot)$  to relate the observed response to covariates and a latent spatial process. For  
145 example,

$$g(u_{s,t}) = \mathbf{X}_{s,t}\mathbf{b} + \omega_s + \epsilon_{s,t}, \quad (1)$$

146 where  $u_{s,t}$  is the expectation at location  $s$  and time  $t$ ,  $\mathbf{X}_{s,t}$  are covariates,  $\mathbf{b}$  represents a vector of  
147 estimated coefficients,  $\omega_s$  is the mean spatial component at location  $s$  (constant through time),  
148 and  $\epsilon_{s,t}$  is the spatiotemporal process at location  $s$  and time  $t$ . The spatiotemporal process  
149 describing  $\epsilon$  is flexible in that it can be removed from the model (leaving a model with a spatial  
150 but no spatiotemporal component), may be independent for each time slice, or modeled with an  
151 autoregressive process (allowing hotspots to persist through time; Ward et al. 2015, Thorson et  
152 al. 2015, Anderson and Ward 2019). Previous applications to marine fishes have either used a  
153 delta-GLMM framework to model presence-absence and positive catch rates separately (Thorson  
154 et al. 2015) or a Tweedie distribution to model total variation in density (Anderson et al. 2019).

155 Within this GLMM framework, non-stationary changes in the spatial predictions through  
156 time can only be modeled with inclusion of dynamic covariates, or by modeling spatiotemporal  
157 variability as an autoregressive spatial process through time. While inclusion of covariates can  
158 improve predictive performance in some cases (e.g., Shelton et al. 2014, Johnson et al. 2019),

159 this requires additional data and can introduce new challenges associated with finding the most  
160 appropriate form of the covariate effect, thus for generality and simplicity we focus here  
161 primarily on a latent variable approach for describing patterns in spatially explicit temporal  
162 trends (hereafter local trends) rather than directly inferring their drivers. Estimates of local trends  
163 may be derived from spatial and spatiotemporal fields post-hoc; however, such post-hoc  
164 estimation results in biases (Fig. S1), specifically a low bias caused by partial pooling, which  
165 effectively pulls the intercept deviations toward the mean. To explicitly account for non-  
166 stationary trends in densities, we extend the above framework to include a trend parameter as an  
167 additional spatial random field for the slopes over time (in the simplest case, each value in the  
168 field represents the spatially-explicit linear trend of the response over the modeled time period).  
169 Extending the model above, this becomes

$$g(u_{s,t}) = \mathbf{X}_{s,t}\mathbf{b} + \omega_s + \epsilon_{s,t} + t \cdot \zeta_s, \quad (2)$$

170 where  $\zeta_s$  represents the spatially varying temporal trend, or local trend. This local trend field can  
171 be thought of as the spatial variability in how a species' density changes through time, which  
172 differentiates such trends from time-independent spatiotemporal random fields (Fig. 1). Note that  
173 this framework could also be extended to model systems in which most spatially explicit  
174 responses are non-linear by either modifying the model structure or by fitting separate models to  
175 each stanza during which a linear trend is suspected.

176

177 *Testing the ability to recover local trends*

178 We conducted a simulation analysis to evaluate our ability to recover an added spatial field  
179 representing the true local trend. Given results from previous work on similar classes of models

180 (Auger-Méthé et al. 2016), we focused our simulations on understanding how the magnitude of  
181 spatiotemporal variation and observation error variation affect our ability to recover the local  
182 trend (details in Supplementary material Appendix 1 methods and Table S1). We also performed  
183 similar sensitivity analyses to verify that the magnitude of spatial variance and local trend would  
184 affect our ability to recover the local trend in predictable ways. All simulations were conducted  
185 following this general outline: for each evaluated (time-invariant) value of spatiotemporal  
186 variation and observation error, we simulated a random spatial field. We then simulated a latent  
187 spatiotemporal process over 10 time steps, using spatial and spatiotemporal components  
188 (modeled as independent from year to year) along with the local trend field. To include  
189 measurement or observation error, we simulated normally distributed observations from this  
190 spatiotemporal process. We then fit a spatial GLMM to the simulated data and assumed the  
191 model structure to be known. We then compared estimated values of the local trend at the  
192 locations of the data with known values to generate statistical summaries (bias [expectation of  
193 difference], variance [sample variance of difference], and Pearson correlations between predicted  
194 and observed values). For each combination of parameter values, we simulated 100 random  
195 datasets.

196

#### 197 *West coast groundfish application*

198 As an example of how the local trend model can be applied to improve the interpretation of  
199 changes in spatial distribution, we fit the local trend model to groundfish data collected from a  
200 fishery-independent survey along the US west coast: the NOAA Fisheries, Northwest Fisheries  
201 Science Center, US West Coast Groundfish Bottom Trawl Survey (Keller et al. 2017) from 2003  
202 to 2018. The annual survey uses a stratified random sampling design, with strata defined by

203 depth and latitude, to estimate population density (in terms of catch per area swept by the net)  
204 along the continental shelf and upper slope (from 55–1280 m depth) of California, Oregon, and  
205 Washington state. Roughly 650 tows (the unit of observation) are performed during two passes  
206 from north to south, typically occurring between late May and the end of October. This survey  
207 represents an ideal case study because it has been used extensively in testing new index  
208 standardization methods for stock assessments (Thorson et al. 2015), is publicly available  
209 (<https://www.nwfsc.noaa.gov/data/map>), and has been used to develop coast-wide indicators,  
210 including shifts in center of gravity (Thorson et al. 2016a). We selected 19 groundfish species to  
211 model in this analysis based on a combination of high commercial landings, market value,  
212 conservation concern, and prevalence in the survey data (Table S2). It is important to note that  
213 the distributions of many of these species extend farther to the north and south. Therefore,  
214 conclusions from these analyses only describe the dynamics of their density distribution within  
215 the survey area, and not their entire range.

216 We fit spatial GLMMs with and without a local trend to each species to evaluate whether  
217 the local trend may be appropriate for modeling how these 19 species change over time. We  
218 allowed both models to include spatial and spatiotemporal components (independent by year,  
219 because preliminary testing indicated that including temporal structure was not typically  
220 supported, as the 95% confidence interval around the estimate of the first-order autoregressive  
221 correlation parameter included 0), depth modeled as a quadratic effect (Thorson et al. 2015), and  
222 year as a factor. Below we describe in detail the full model including the local trend.

223 Because of the positive continuous nature of the recorded fish densities combined with  
224 some zeros, we modeled the response  $y_{s,t}$  (catch per unit effort [CPUE] at point in space  $s$  and

225 time  $t$ ) with a Tweedie distribution and a log link (Tweedie 1984, Dunn and Smyth 2005,  
 226 Anderson et al. 2019):

$$\begin{aligned} y_{s,t} &\sim \text{Tweedie}(\mu_{s,t}, p, \phi), 1 < p < 2, \\ \mu_{s,t} &= \exp(\alpha_t + \beta_1 D_{s,t} + \beta_2 D_{s,t}^2 + \omega_s + \epsilon_{s,t} + \zeta_s t), \\ \boldsymbol{\omega} &\sim \text{MVNormal}(\mathbf{0}, \boldsymbol{\Sigma}_{\omega}), \\ \boldsymbol{\epsilon}_t &\sim \text{MVNormal}(\mathbf{0}, \boldsymbol{\Sigma}_{\epsilon}), \\ \boldsymbol{\zeta} &\sim \text{MVNormal}(\mathbf{0}, \boldsymbol{\Sigma}_{\zeta}), \end{aligned} \quad (3)$$

227 where  $\mu$  represents the mean,  $p$  represents the power parameter, and  $\phi$  represents the dispersion  
 228 parameter. The  $\alpha_t$  parameters represent independent means estimated for each year, and  $\beta_1$  and  
 229  $\beta_2$  represent coefficients for log depth ( $D$ ) and log depth squared ( $D^2$ ). The symbols  $\omega_s$  and  $\epsilon_{s,t}$   
 230 represent spatial and spatiotemporal random effects (respectively) drawn from Gaussian Markov  
 231 random fields (Cressie and Wikle 2011) with covariance matrices  $\boldsymbol{\Sigma}_{\epsilon}$  and  $\boldsymbol{\Sigma}_{\omega}$ . The symbol  $\zeta_s$   
 232 represents the spatially varying coefficients that represent local trends through time, also drawn  
 233 from Gaussian Markov random fields. Time,  $t$ , is entered into the model for multiplication with  
 234  $\zeta_s$  after centering it by its mean value. All three random fields have covariance matrices  
 235 constrained by anisotropic Matérn covariance functions with independent scales but shared  $\kappa$   
 236 parameters controlling the rate of decay of spatial correlation with distance (Cressie and Wikle  
 237 2011, Thorson et al. 2015).

238 We approximated the continuous random fields using a triangulated mesh with vertices at  
 239 350 “knots” (Rue et al. 2009, Lindgren et al. 2011) as calculated with the INLA R package (Rue  
 240 et al. 2009) and used bilinear interpolation to predict at locations between the knots. We found  
 241 the minimum log likelihood using the R nlmrb optimization routine with Template Model  
 242 Builder (TMB; Kristensen et al. 2016) implementing the Laplace approximation to the marginal  
 243 likelihood. TMB uses the generalized delta-method to calculate standard errors. We used bilinear

244 interpolation to project predictions at the knot locations to the data locations. Specifically, we fit  
245 all models in R version 3.5.3 (R Core Team 2019) using the package sdmTMB (Anderson et al.  
246 2019, 2020) which interfaces automatic differentiation in Template Model Builder (Kristensen et  
247 al. 2016) with INLA (Rue et al. 2009).

248 To compare models with different random effect structures (with and without the local  
249 trend field), we used restricted maximum likelihood (REML, Zuur et al. 2009) to generate  
250 Akaike's Information Criterion values for each model (AIC, Akaike 1973). AIC is a relative  
251 measure of goodness-of-fit that is penalized by the number of model parameters. Using AIC as a  
252 model screening tool, we found broad support for the inclusion of the local trend for these 19  
253 species, with the trend model generating lower AIC values in 17 of the 19 cases, and AIC scores  
254 differing by less than two in the remaining two cases (Table S3). To verify that AIC was  
255 effective at selecting the model most consistent with the data-generating process, we performed  
256 parallel contrasts (between models with and without the local trend) using simulated data.

257 Given the evidence supporting the local trend model as the most parsimonious model, we  
258 used this model structure to evaluate changes in species density distributions over time. To  
259 obtain a smooth surface of predicted density across the footprint of the survey area (Fig. 2), we  
260 predicted density using a composite of depth layers defined by NOAA bathymetry data  
261 (<https://www.ngdc.noaa.gov/mgg/coastal/crm.html>). These data were spatially aggregated using  
262 bilinear interpolation to match the resolution of the survey sampling grid (~2.8 x 3.7 km), which  
263 is the spatial resolution we used for all analyses. We implemented a number of diagnostics using  
264 spot checks on these predictions and model fits to further analyze whether a local trend was  
265 appropriate (e.g., examining spatial patterns in residuals and the estimated spatiotemporal  
266 component).

267

268 *Using local trends as indicators of change*

269 We compared inferences of changes in species density distributions obtained from  
270 metrics calculated on a spectrum of spatial resolution to demonstrate the utility of understanding  
271 fine-scale temporal trends. Quantifying change at multiple spatial scales has implications for the  
272 management of marine fishes and has utility as a spatial indicator within the California Current  
273 ecosystem. Specifically, we compared the fine-scale interpretation of the local trend and mean  
274 predicted density over all years to coarse-scale interpretations of: 1) the local trend, 2) regional  
275 COGs and 3) coastwide COG calculated from predicted densities  $y$  for each location  $s$  and time  $t$   
276 ( $COG_t = \frac{\sum y_{s,t} L_s}{\sum y_{s,t}}$ , where  $L_s$  is the  $y$  coordinate of location  $s$ ). We use the mean predicted density  
277 over time as a benchmark for describing how species' distributions change because this can be  
278 interpreted as a "weight" on the local trend, where the product of the two defines the absolute  
279 magnitude of the change in density over time.

280 We evaluated whether local trend estimates from our model can be used to identify  
281 discrete areas of change that may reflect stock structure. One approach among many possible  
282 options for doing this is to apply post-hoc cluster analyses to model outputs or covariates; for our  
283 groundfish application, we used the partitioning around medoids (PAM) algorithm with  
284 estimation of the number of clusters to demonstrate a possible framework for boundary detection  
285 to be used with other system information to define appropriate spatial scales for summarizing  
286 monitoring data (implemented with R packages "fpc" and "cluster", Hennig 2019, Maechler et  
287 al. 2019). PAM is a robust clustering algorithm that minimizes the sum of Euclidean  
288 dissimilarities (root of sum-of-squares of differences) between observations and cluster values

289 (Reynolds et al. 2006, Kaufman and Rousseeuw 2009). We used latitude and the predicted local  
290 trends as clustering variables given that the majority of the contrast in dynamics along the US  
291 west coast is in the latitudinal direction. For other applications, additional metrics could also be  
292 included in clustering including longitude, habitat features, environmental covariates, or human  
293 impacts such as fisheries removals. We chose the number of clusters (constrained between 1 and  
294 10) that maximized the average silhouette width across all predictions for a given species  
295 (Kaufman and Rousseeuw 2009). Code and data necessary to replicate all above analyses are  
296 included in the repository for this project (<https://github.com/fate-spatialindicators/spatial-trend>).

297

## 298 **Results**

### 299 *Simulation testing*

300 Results from our simulation indicated that, as expected, both observation error variation and  
301 spatiotemporal variation degraded our ability to estimate the true local trend (Fig. 3). When both  
302 variance parameters were small, estimates were precisely estimated and unbiased; however, large  
303 values of either limited the ability to recover the trend (Fig. 3). Results of further sensitivity  
304 analysis were also as expected (Fig. S2), with spatial variation having no effect on local trend  
305 estimates, while estimates of the local trend were only poor when the variation of the local trend  
306 field was extremely low (i.e., the signal was barely present and obscured by variation in other  
307 components, causing low correlation between estimated and true local trends; Fig. S2f).  
308 Furthermore, we found that the correct model (the model including the local trend) was easily  
309 distinguished by model selection using AIC except when observation error or spatiotemporal  
310 variation was extremely high, or when the local trend variance was extremely low (Fig. S3).

311

312 *West coast groundfish application*

313 Predictions of the spatially explicit temporal trend from the local trend model revealed intricate  
314 fine-scale spatial structure and rates of change of species in the west coast groundfish  
315 community. Our cluster analysis of the estimated local trend and latitude helped to delineate  
316 areas with the greatest relative rate of change in density over time. For the majority (58%) of  
317 species, at least one of the breaks between local trend clusters occurred at a latitude within  
318 100km of the two predominant biogeographic breaks in this ecosystem: Point Conception in  
319 southern California and Cape Mendocino in northern California (Fig. 4). Furthermore, all species  
320 had at least one cluster break falling at latitudes between these two biogeographic boundaries and  
321 79% of species had at least half of their cluster breaks in this area. However, there was  
322 variability among species in the precise location of the boundaries of the local trend clusters.  
323 Results were similar, yet clusters were less spatially contiguous, when clustering on only the  
324 local trend without latitude (Fig. S4). Given the general proximity between trend cluster breaks  
325 and the established biogeographic boundaries, we chose to evaluate the latitudinal center of  
326 gravity (COG) within each biogeographic region (rather than within each species-specific local  
327 trend cluster) to compare with the coastwide COG. Early exploration indicated that results were  
328 qualitatively similar between these two approaches for defining the unit on which to compute  
329 COGs; however, we chose not to compute COGs by local trend cluster over concerns that this  
330 could minimize and obscure distribution shifts (e.g., if density is changing uniformly over time  
331 within a cluster, one would expect the COG of that cluster to remain relatively constant).

332 We highlight results for six groundfish species with unique distributional responses (Fig.  
333 5; see Fig. S5 for results from additional species and Fig. S6 for predicted density distributions

334 for all 19 species). Within each of the six species, there was support for 2–3 trends (Fig. 5;  
335 second column). Comparison of the local trend predictions and clusters (Fig. 5; first two  
336 columns) and the mean density from the full model (Fig. 5; third column) revealed how several  
337 unique patterns of regional relationships can contribute to nuanced and difficult to detect broad-  
338 scale distributional changes including northward, southward, and bi-directional (convergent or  
339 divergent) density shifts, in addition to localized offshore shifts. Furthermore, the interpretation  
340 of the distributional change often varied between spatial scales of metrics. Typically, inference  
341 differed the most between the fine-scale map-based interpretation of the local trend and the  
342 coastwide COG. The map of estimated mean density allows one to visually weight the local  
343 trend map to better understand where absolute changes in density are greatest.

344 Examining the predictions of the local trend and density indicated that arrowtooth  
345 flounder (*Atheresthes stomias*) had a southward density shift and shortspine thornyhead  
346 (*Sebastolobus alascanus*) had a northward shift, yet the COG inferences differed to some degree  
347 between species. The predicted density indicated that the majority of arrowtooth flounder (Fig. 5,  
348 first row) was in the northern region, yet the local trend pattern indicates that their density is  
349 increasing at the highest rate in the central region. Combined, these regional results suggest a  
350 southward shift driven by increases at the southern range edge, similar to the traveling wave  
351 pattern demonstrated by many species invasions. The time series of the coast-wide COG (black  
352 line in last column of Fig. 5) is in agreement of a southward shift, yet the interpretation is not as  
353 clear because the coast-wide pattern is heavily weighted by the high densities in the far northern  
354 portion of the study area. When the COG from each biogeographic region is calculated (colored  
355 lines in last column of Fig. 5), we can see that coast-wide COG has been driven further south in  
356 the latter half of the time series by decreases in the COG in the central region while the northern

357 COG had almost no trend, providing additional support for the possibility that the change is due  
358 to increased density or southward shifts in the central region.

359 For other species in our analysis, even the region-specific COG does not accurately  
360 capture the nuanced spatial changes described by the local trend field. For example, shortspine  
361 thornyhead is distributed coast-wide, yet their density is increasing fastest in the north-central  
362 area and decreasing in the south and within some isolated patches in the far northern end of the  
363 region (Fig. 5, last row, left column). In this case, the coast-wide COG indicates a northward  
364 distribution shift, yet the region-specific COG indicates converging trends, perhaps indicative of  
365 contraction of the core range: slightly southward shifting of the northern region and slight  
366 northward shift in the central region. Thus, the interpretation from the COGs at both scales are  
367 relatively consistent with the fine-scale interpretation of the local trend, yet these coarse-scale  
368 metrics still mask underlying patterns, in this case the decreased density in the southern region.

369 Other species demonstrated additional patterns of changes in spatial distribution of  
370 density and contrasting inference among metrics, including bocaccio rockfish (*Sebastes*  
371 *paucispinis*), English sole (*Parophrys vetulus*), petrale sole (*Eopsetta jordani*), and sablefish  
372 (*Anoplopoma fimbria*). Bocaccio were typically more abundant in the southern and central areas  
373 yet were experiencing the fastest increases in density in the north, indicating a northward density  
374 shift. These observations contrast with those from the COG, where the coast-wide COG for  
375 bocaccio was highly variable with either no trend or a very slight southward trend, and the COG  
376 of the northern region indicates a southward shift in some years. Divergent density shifts were  
377 observed for English sole and, to some extent, petrale sole. English sole were typically present in  
378 relatively similar densities coast-wide, yet the local trend indicated that densities were increasing  
379 fastest at the northern and southern ends of the region. However, the coast-wide COG reveals

380 only a slight southward shift, while the region-specific COGs show only a slight northward shift  
381 in the northern region. Petrale sole had a complex local trend field, increasing fastest in the north  
382 with the exception of isolated declining patches on the inshore side. These changes are somewhat  
383 consistent with the coast-wide COG indicating a slight northward trend amidst moderate  
384 interannual variability. However, COGs of the northern and central regions—where petrale sole  
385 are typically most prevalent—indicated a divergent pattern, in which densities were shifting  
386 northward in the northern region and slightly southward in the central region. Finally, no obvious  
387 directional shift in density was apparent in the local trend for sablefish, yet the coast-wide COG  
388 time series indicated that a northward shift had occurred in the most recent 5–6 years. The  
389 region-specific COG indicates that this was driven by density changes in the northern and to  
390 some extent central regions. Thus, depending on the evidence used, one could either conclude  
391 that there was a recent northward density shift, or simply an increase in productivity or  
392 aggregation near the core of the range within the north-central area.

393

#### 394 **Discussion**

395 The complex spatial distribution of biotic and abiotic drivers of population productivity and  
396 habitat suitability in ecosystems suggests that fine-scale descriptors may provide a more accurate  
397 representation of changes in species distributions than global indicators calculated across an  
398 entire region. Here, we introduced a new approach to modeling and summarizing spatially  
399 referenced time series data on species population densities to calculate area-specific trends in  
400 population size. Our approach was able to recover local trends in simulated data and reveal  
401 nuanced local trends in the dynamics of 19 marine fishes off the west coast of the USA that often  
402 differed from conventional descriptors of larger scale distribution shifts (Woillez et al. 2009,

403 Pinsky et al. 2013, Thorson et al. 2016a). Furthermore, the ability of our models to detect  
404 geographic boundaries between regions with different trends was supported as these boundaries  
405 were often congruent with known biogeographic breaks (yet we acknowledge that this may be  
406 influenced by assumptions affecting the optimization of the number of clusters and other factors  
407 that require deeper investigation to strengthen this initial finding). Therefore, boundary detection  
408 techniques applied to a local trend field may be valuable for helping to define appropriate spatial  
409 scales for summarizing monitoring products (such as abundance time series) or regulating the  
410 spatial allocation of human impacts (e.g., allowable take of animals or plants), especially in cases  
411 where little other information on spatial population and community structure is available.  
412 Furthermore, we note that the local trend model described here has potential for broad  
413 applications to a variety of other data types beyond population density (e.g., spatial patterns of  
414 temperature variability) and other systems (as an extension of existing applications, e.g.,  
415 Banerjee et al. 2008, Finley et al. 2009, Latimer et al. 2009, Cressie and Wikle 2011, Thorson et  
416 al. 2016b, Hocking et al. 2018)

417 Our simulations and application of the local trend model indicate that our proposed  
418 approach can improve estimation and communication of spatially varying temporal trends in  
419 population density. In particular, our application to marine fish survey data indicated that models  
420 including a local trend field were more parsimonious than those without a local trend. This result  
421 is consistent with a recent study incorporating a spatially varying influence of an oceanographic  
422 index on groundfish distributions in the eastern Bering Sea (Thorson 2019a). Furthermore,  
423 according to our simulations the estimated local trends were less biased than those estimated  
424 post-hoc from predictions of a model without the local trend field. However, the local trend  
425 model is somewhat sensitive to observation error and spatiotemporal variation. Such sources of

426 variation can obscure the local trend, yet this is to be expected in the same way that any trend is  
427 less detectable given noisier data (Weatherhead et al. 1998). Therefore, our method is likely most  
428 skillful at detecting spatial structure in population or community dynamics from observations  
429 with precise measurement within systems with low temporal variation in spatial structure (e.g.,  
430 those consisting of species with higher longevity, generation time, and site fidelity, and lower  
431 rates of movement and variation in dispersal paths). We expect that the predictions in our  
432 example application in this study are robust to the sensitivity of the method to spatiotemporal  
433 variation because the estimated spatiotemporal variance is much lower than the spatial variance  
434 for groundfish species in this system. Observation error in trawl surveys can include a wide  
435 range of values as a result of variance in sampling efficiency (Kotwicki and Ono 2019), but  
436 relating such values to the observation error scale parameter evaluated in our simulations  
437 requires additional research. Additional ways to constrain the variance parameters, such as  
438 developing informative Bayesian priors from similar surveys might extend the detectability of  
439 local trend structure over the models used here.

440 We showed how inference about shifts in species' population density depend on the  
441 spatial scale at which they are summarized. When we applied the local trend model to marine  
442 fishes, the resulting maps of the local trend and density from the model revealed nuanced  
443 patterns of heterogeneity and directional change in groundfish density (COG; this study, Thorson  
444 et al. 2016a). Taking the predicted density to represent the underlying spatial heterogeneity, the  
445 local trend random field conveyed fine-scale information about potential range dynamics that  
446 were masked when evaluating coast-wide COG time series. The disparity of inference was  
447 greatest in cases where density was increasing fastest at opposing ends of a range, density was  
448 spatially diverging, or where density among patches were converging toward the center of the

449 distribution. Furthermore, when examining only the coast-wide COG, one is unable to  
450 differentiate between shifts due to an increase in density in one area or a decrease in density in  
451 another area.

452 For complex ecosystems such as the US west coast, and other coastal upwelling systems  
453 where physical variables like temperature do not follow a simple monotonic gradient over broad  
454 geographic scales, it may be too simplistic to expect clear coast-wide trends in COG across  
455 multiple species as a result of climate change. These coast-wide patterns are observed in systems  
456 with broader continental shelves such as the northeast US (Pinsky et al. 2013, Kleisner et al.  
457 2016) where the major boundary currents are far from the coast. However, along coastlines with  
458 narrower continental margins, such as the US west coast, fish may be able to find equivalent  
459 temperatures by moving much shorter distances perpendicular to the shelf break (Li et al. 2019).  
460 Furthermore, population and community density distributions are inherently patchy, particularly  
461 for species associated with patchy reef habitats, meaning that detecting a redistribution over time  
462 may require careful examination of the microstructure of density distribution rather than a  
463 region-wide shift in mean density distribution. We encourage future research on species  
464 distribution shifts that begins with more specific and nuanced hypotheses regarding the expected  
465 response at shorter and perhaps longer time scales than those explored here, as spatially-explicit  
466 trends are likely to differ between intra-annual, inter-annual, and inter-decadal time scales. For  
467 example, event-scale analyses of the local trend could help test how different species population  
468 density distributions respond as a result of movement or demography to disease outbreaks,  
469 intensive harvesting, or extreme climate events such as marine heat waves. If climate change  
470 causes a global intensification of upwelling over longer time scales as some researchers predict  
471 (Bakun et al. 2010), one could hypothesize that density distributions will become patchier over

472 time in response to increasing contrast in local physical conditions, or that distributions will shift  
473 deeper as larvae are transported further offshore before settling.

474 The future of environmental conservation and natural resource management relies on  
475 greater incorporation of spatial information into models that inform such policies and into the  
476 decision-making process itself (Berger et al. 2017, Lowerre-Barbieri et al. 2019). By defining the  
477 geography of population trends and the breaks between clusters of locations with similar trends,  
478 our modeling framework provides a data-driven method to objectively define the spatial scale  
479 and boundaries for summarizing monitoring data and structuring these inputs to resource  
480 management models. This is an important advancement over non-spatial resource assessments or  
481 the reliance on the use of jurisdictional boundaries to structure resource assessments. Our vision  
482 is that these and subsequent methods for boundary detection will aid the development of spatial  
483 resource assessment models and stimulate further applications of such approaches to more  
484 disparate management solutions such as invasive species management. Furthermore, extensions  
485 of the methods presented here may lead to the creation and improvement of spatial indicators for  
486 monitoring factors affecting emergent ecological properties (e.g., Barnett et al. 2019 and  
487 references therein). Novel indicators of ecological stability could arise from metrics of the spatial  
488 structure of temporal trends or oscillations in population density (Kéfi et al. 2014, Walter et al.  
489 2017), by drawing on the evidence that spatial heterogeneity can increase population and  
490 community stability by disrupting synchrony across space or among species (Huffaker 1958,  
491 Tilman and Kareiva 1997, Hassell 2000).

**492    Figure Captions**

493    Figure 1. Visualization of how the spatial distribution of population density changes over time  
494    when the temporal response differs among locations. Predictions are shown from the spatial and  
495    temporal random effects of a GLMM with (top row) and without (bottom row) a spatially  
496    varying temporal trend (i.e., local trend). Each panel shows a field representing the spatial  
497    variation in population density, and the columns show how these patterns change over time (e.g.,  
498    five years). When a spatially varying temporal trend is present, some regions develop  
499    systematically higher (red) or lower (blue) density over time. In contrast, when a spatially  
500    varying temporal trend is absent, spatial deviations from year-to-year are independent. For this  
501    example, we have omitted all other sources of variability and error for simplicity.

502

503    Figure 2. Map of the bathymetry within the US west coast groundfish bottom trawl survey  
504    footprint. Cape Mendocino and Point Conception are labeled to represent the latitudinal  
505    boundaries between known predominant biogeographic regions (N.B. there is also more limited  
506    evidence for additional or alternative biogeographic breaks, e.g., Cape Blanco, the westernmost  
507    point in Oregon).

508

509    Figure 3. Simulation testing the effects of observation error and spatiotemporal variation on the  
510    ability to recover the local trend. The symbols  $\theta$  and  $\hat{\theta}$  refer to the local trend random effect  
511    values at each location  $\zeta_s$  and their estimate, respectively. Each violin represents the distribution  
512    of location by location comparisons from 100 simulations and the dots represent the median  
513    value. In all cases, the standard deviation of the non-varying parameter is held at 0.01, while  $\sigma$

514 varies along  $\{0.01, 0.25, 0.5, 0.75\}$ . Note that these results were also computed for  $\sigma = 1$  (see  
515 Table S1), yet are omitted here as they were very similar to results from  $\sigma = 0.75$ .

516

517 Figure 4. Strip plot showing each unique cluster of latitude and local trend (slope over time) by  
518 species. Each set of points associated with a given cluster are represented by a different column  
519 and colored by their deviation from the mean coast-wide trend for a given species. Grey points  
520 represent clusters from which the trend was within 0.01 of the mean coast-wide trend. Horizontal  
521 black lines represent approximate positions of known biogeographic breaks: Cape Mendocino,  
522 California, in the north; Point Conception, California, in the south. Horizontal gray shading  
523 represents a buffer of 100km around each biogeographic boundary, which provide a benchmark  
524 for the proximity statistics described in the main text.

525

526 Figure 5. Spatial and temporal patterns of predicted density for selected species along the US  
527 west coast. Panels depict model outputs within the study area (shown in further detail in Figure  
528 2), where the thin black polygon in maps is the land boundary of the US west coast. The first  
529 column shows maps of the predicted local trend (slope of log density across years). The second  
530 shows how each spatial location groups with a unique cluster of latitude and local trend, where  
531 each color represents a cluster. The first panel also shows how the latitudinal boundaries of  
532 established biogeographic breaks (thick black horizontal lines) separate the study area into three  
533 regions: North of Cape Mendocino, California; South of Point Conception, California; and  
534 between these two landmarks (central). The third column represents the mean density over all  
535 years (in units of  $\text{kg km}^{-2}$  on a log scale). The fourth column shows the time series of the center  
536 of gravity (COG), or latitude weighted by density, with 95% confidence intervals. The black line

537 with grey interval represents the COG calculated from predicted densities coast-wide, whereas  
538 the colored lines represent the COGs for each unique biogeographic region. Line color represents  
539 the proportion of a species' relative biomass in a given region.

For Review Only

540 **References**

- 541 Akaike, H. 1973. Information theory and an extension of the maximum likelihood principle. -  
542 2nd Int. Symp. Inf. Theory, pp. 267–281.
- 543 Anderson, S. C. and Ward, E. J. 2019. Black swans in space: modeling spatiotemporal processes  
544 with extremes. - Ecology 100: e02403.
- 545 Anderson, S. C. et al. 2019. A reproducible data synopsis for over 100 species of British  
546 Columbia groundfish. - DFO Can Sci Advis Sec Res Doc 2019/041 [http://www.dfo-  
547 mpo.gc.ca/csas-sccs/Publications/ResDocs-DocRech/2019/2019\\_041-eng.html](http://www.dfo-mpo.gc.ca/csas-sccs/Publications/ResDocs-DocRech/2019/2019_041-eng.html)
- 548 Anderson, S. C. et al. 2020. sdmTMB: Spatiotemporal Species Distribution GLMMs with  
549 'TMB'. <https://github.com/seananderson/sdmTMB>
- 550 Auger-Méthé, M. et al. 2016. State-space models' dirty little secrets: even simple linear Gaussian  
551 models can have estimation problems. - Sci. Rep. 6: 26677.
- 552 Bakun, A. et al. 2010. Greenhouse gas, upwelling-favorable winds, and the future of coastal  
553 ocean upwelling ecosystems. - Glob. Change Biol. 16: 1213–1228.
- 554 Banerjee, S. et al. 2008. Gaussian predictive process models for large spatial data sets. - J. R.  
555 Stat. Soc. Ser. B Stat. Methodol. 70: 825–848.
- 556 Barnett, L. A. K. et al. 2019. Dynamic spatial heterogeneity reveals interdependence of marine  
557 faunal density and fishery removals. - Ecol. Indic. 107: 105585.
- 558 Berger, A. M. et al. 2017. Space oddity: The mission for spatial integration. - Can. J. Fish.  
559 Aquat. Sci. 74: 1698–1716.
- 560 Chen, J. et al. 2004. Estimation of fish abundance indices based on scientific research trawl  
561 surveys. - Biometrics 60: 116–123.

- 562 Connor, T. et al. 2019. Interactive spatial scale effects on species distribution modeling: The case  
563 of the giant panda. - *Sci. Rep.* 9: 14563.
- 564 Cressie, N. and Wikle, C. K. 2011. Statistics for spatio-temporal data. - John Wiley & Sons.
- 565 Dunn, P. K. and Smyth, G. K. 2005. Series evaluation of Tweedie exponential dispersion model  
566 densities. - *Stat. Comput.* 15: 267–280.
- 567 Efford, M. 2004. Density estimation in live-trapping studies. - *Oikos* 106: 598–610.
- 568 Efford, M. G. 2011. Estimation of population density by spatially explicit capture–recapture  
569 analysis of data from area searches. - *Ecology* 92: 2202–2207.
- 570 Elith, J. and Leathwick, J. R. 2009. Species distribution models: Ecological explanation and  
571 prediction across space and time. - *Annu. Rev. Ecol. Evol. Syst.* 40: 677–697.
- 572 Elith, J. et al. 2010. The art of modelling range-shifting species. - *Methods Ecol. Evol.* 1: 330–  
573 342.
- 574 Finley, A. O. et al. 2009. Improving the performance of predictive process modeling for large  
575 datasets. - *Comput Stat Data Anal* 53: 2873–2884.
- 576 Harvey, C. et al. 2018. Ecosystem Status Report of the California Current for 2018: A Summary  
577 of Ecosystem Indicators Compiled by the California Current Integrated Ecosystem  
578 Assessment Team CCIEA. NOAA Tech. Memo. NMFS-NWFSC-149.
- 579 Hassell, M. 2000. The spatial and temporal dynamics of host-parasitoid interactions. - Oxford  
580 University Press.
- 581 Hennig, C. 2019. *fpc*: Flexible Procedures for Clustering. R package version 2.2-1.  
582 <https://CRAN.R-project.org/package=fpc>
- 583 Hitch, A. T. and Leberg, P. L. 2007. Breeding distributions of North American bird species  
584 moving north as a result of climate change. - *Conserv. Biol.* 21: 534–539.

- 585 Hocking, D. J. et al. 2018. A geostatistical state-space model of animal densities for stream  
586 networks. - *Ecol. Appl.* 28: 1782–1796.
- 587 Huffaker, C. B. 1958. Experimental studies on predation: dispersion factors and predator-prey  
588 oscillations. - *Hilgardia* 27: 795–835.
- 589 Johnson, K. F. et al. 2019. Investigating the value of including depth during spatiotemporal index  
590 standardization. - *Fish. Res.* 216: 126–137.
- 591 Kaufman, L. and Rousseeuw, P. J. 2009. Finding groups in data: an introduction to cluster  
592 analysis. - John Wiley & Sons.
- 593 Kéfi, S. et al. 2014. Early warning signals of ecological transitions: methods for spatial patterns.  
594 - *PloS One* 9: e92097.
- 595 Keller, A. A. et al. 2017. The Northwest Fisheries Science Center's West Coast Groundfish  
596 Bottom Trawl Survey: History, design, and description. NOAA Tech. Memo. NMFS-  
597 NWFSC-136.
- 598 Kleisner, K. M. et al. 2016. The effects of sub-regional climate velocity on the distribution and  
599 spatial extent of marine species assemblages. - *PLOS ONE* 11: e0149220.
- 600 Kotwicki, S. and Ono, K. 2019. The effect of random and density-dependent variation in  
601 sampling efficiency on variance of abundance estimates from fishery surveys. - *Fish Fish.*  
602 20: 760–774.
- 603 Kristensen, K. et al. 2016. TMB: Automatic differentiation and Laplace approximation. - *J. Stat.*  
604 *Softw.* 70: 1–21.
- 605 Latimer, A. M. et al. 2009. Hierarchical models facilitate spatial analysis of large data sets: a  
606 case study on invasive plant species in the northeastern United States. - *Ecol. Lett.* 12:  
607 144–154.

- 608 Lenoir, J. et al. 2008. A significant upward shift in plant species optimum elevation during the  
609 20th century. - *Science* 320: 1768.
- 610 Levin, S. A. 1992. The problem of pattern and scale in ecology: the Robert H. MacArthur award  
611 lecture. - *Ecology* 73: 1943–1967.
- 612 Levin, L. A. et al. 2010. The roles of habitat heterogeneity in generating and maintaining  
613 biodiversity on continental margins: an introduction. - *Mar. Ecol. Prog. Ser.* 31: 1–5.
- 614 Li, L. et al. 2019. Subregional differences in groundfish distributional responses to anomalous  
615 ocean bottom temperatures in the northeast Pacific. - *Glob. Change Biol.* 25: 2560–2575.
- 616 Lindgren, F. et al. 2011. An explicit link between Gaussian fields and Gaussian Markov random  
617 fields: the stochastic partial differential equation approach. - *J. R. Stat. Soc. Ser. B Stat.*  
618 *Methodol.* 73: 423–498.
- 619 Link, J. S. et al. 2002. Marine ecosystem assessment in a fisheries management context. - *Can. J.*  
620 *Fish. Aquat. Sci.* 59: 1429–1440.
- 621 Lowerre-Barbieri, S. K. et al. 2019. Preparing for the future: integrating spatial ecology into  
622 ecosystem-based management. - *ICES J. Mar. Sci.* 76: 467–476.
- 623 Maechler, M. et al. 2019. *cluster*: Cluster analysis basics and extensions. R package version  
624 2.1.0.
- 625 Nicholson, M. D. and Jennings, S. 2004. Testing candidate indicators to support ecosystem-  
626 based management: the power of monitoring surveys to detect temporal trends in fish  
627 community metrics. - *ICES J. Mar. Sci.* 61: 35–42.
- 628 Pinsky, M. L. et al. 2013. Marine taxa track local climate velocities. - *Science* 341: 1239–1242.
- 629 R Core Team 2019. R: A language and environment for statistical computing. - R Foundation for  
630 Statistical Computing.

- 631 Reynolds, A. P. et al. 2006. Clustering rules: A comparison of partitioning and hierarchical  
632 clustering algorithms. - *J. Math. Model. Algorithms* 5: 475–504.
- 633 Rice, J. C. and Garcia, S. M. 2011. Fisheries, food security, climate change, and biodiversity:  
634 characteristics of the sector and perspectives on emerging issues. - *ICES J. Mar. Sci.* 68:  
635 1343–1353.
- 636 Royle, J. A. and Young, K. V. 2008. A hierarchical model for spatial capture–recapture data. -  
637 *Ecology* 89: 2281–2289.
- 638 Royle, J. A. et al. 2013. Spatial capture-recapture. - Academic Press.
- 639 Rue, H. et al. 2009. Approximate Bayesian inference for latent Gaussian models by using  
640 integrated nested Laplace approximations. - *J. R. Stat. Soc. Ser. B Stat. Methodol.* 71:  
641 319–392.
- 642 Ruiz-Cárdenas, R. et al. 2012. Direct fitting of dynamic models using integrated nested Laplace  
643 approximations — INLA. - *Comput. Stat. Data Anal.* 56: 1808–1828.
- 644 Sagarin, R. D. and Gaines, S. D. 2002. The ‘abundant centre’ distribution: to what extent is it a  
645 biogeographical rule? - *Ecol. Lett.* 5: 137–147.
- 646 Sagarin, R. D. et al. 2006. Moving beyond assumptions to understand abundance distributions  
647 across the ranges of species. - *Trends Ecol. Evol.* 21: 524–530.
- 648 Shelton, A. O. et al. 2014. Spatial semiparametric models improve estimates of species  
649 abundance and distribution. - *Can. J. Fish. Aquat. Sci.* 71: 1655–1666.
- 650 Stock, B. C. et al. 2019. Comparing predictions of fisheries bycatch using multiple  
651 spatiotemporal species distribution model frameworks. - *Can. J. Fish. Aquat. Sci.* 77:  
652 146–163.

- 653 Thorson, J. T. 2019a. Measuring the impact of oceanographic indices on species distribution  
654 shifts: The spatially varying effect of cold-pool extent in the eastern Bering Sea. -  
655 Limnol. Oceanogr. 64: 2632–2645.
- 656 Thorson, J. T. 2019b. Guidance for decisions using the Vector Autoregressive Spatio-Temporal  
657 (VAST) package in stock, ecosystem, habitat and climate assessments. - Fish. Res. 210:  
658 143–161.
- 659 Thorson, J. T. and Barnett, L. A. K. 2017. Comparing estimates of abundance trends and  
660 distribution shifts using single- and multispecies models of fishes and biogenic habitat. -  
661 ICES J. Mar. Sci. 74: 1311–1321.
- 662 Thorson, J. T. et al. 2015. Geostatistical delta-generalized linear mixed models improve  
663 precision for estimated abundance indices for West Coast groundfishes. - ICES J. Mar.  
664 Sci. 72: 1297–1310.
- 665 Thorson, J. T. et al. 2016a. Model-based inference for estimating shifts in species distribution,  
666 area occupied and centre of gravity. - Methods Ecol. Evol. 7: 990–1002.
- 667 Thorson, J. T. et al. 2016b. Joint dynamic species distribution models: A tool for community  
668 ordination and spatio-temporal monitoring. - Glob. Ecol. Biogeogr. 25: 1144–1158.
- 669 Tilman, D. and Kareiva, P. M. 1997. Spatial ecology: The role of space in population dynamics  
670 and interspecific interactions. - Princeton University Press.
- 671 Tingley, M. W. and Beissinger, S. R. 2009. Detecting range shifts from historical species  
672 occurrences: new perspectives on old data. - Trends Ecol. Evol. 24: 625–633.
- 673 Tweedie, M. C. 1984. An index which distinguishes between some important exponential  
674 families. - Stat. Appl. New Dir. Proc. Indian Stat. Inst. Gold. Jubil. Int. Conf. Eds J K  
675 Ghosh J Roy 579: 579–604.

- 676 Walter, J. A. et al. 2017. The geography of spatial synchrony. - *Ecol. Lett.* 20: 801–814.
- 677 Ward, E. J. et al. 2015. Using spatiotemporal species distribution models to identify temporally  
678 evolving hotspots of species co-occurrence. - *Ecol. Appl.* 25: 2198–2209.
- 679 Weatherhead, E. C. et al. 1998. Factors affecting the detection of trends: Statistical  
680 considerations and applications to environmental data. - *J. Geophys. Res. Atmospheres*  
681 103: 17149–17161.
- 682 Woillez, M. et al. 2009. Notes on survey-based spatial indicators for monitoring fish populations.  
683 - *Aquat. Living Resour.* 22: 155–164.
- 684 Yackulic, C. B. et al. 2013. Presence-only modelling using MAXENT: when can we trust the  
685 inferences? 4: 236–243.
- 686 Zuur, A. F. et al. 2009. Mixed effects models and extensions in ecology with R, 1st edition. -  
687 Springer.

Time step

Ecography

2

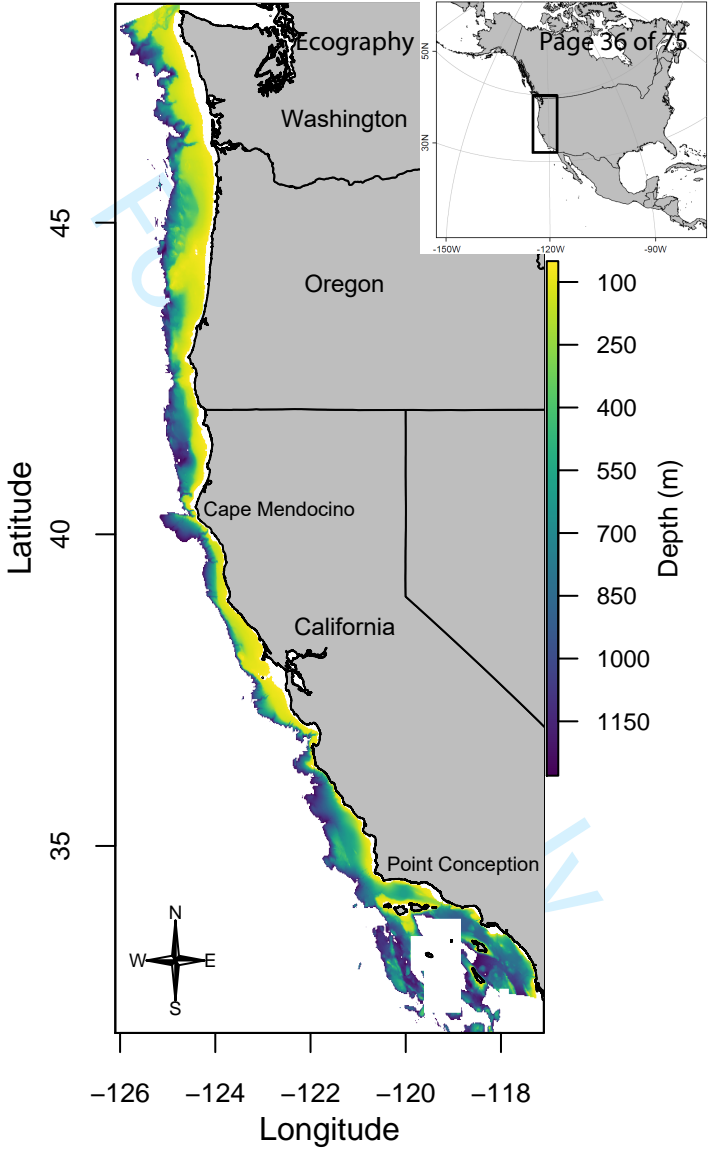
4

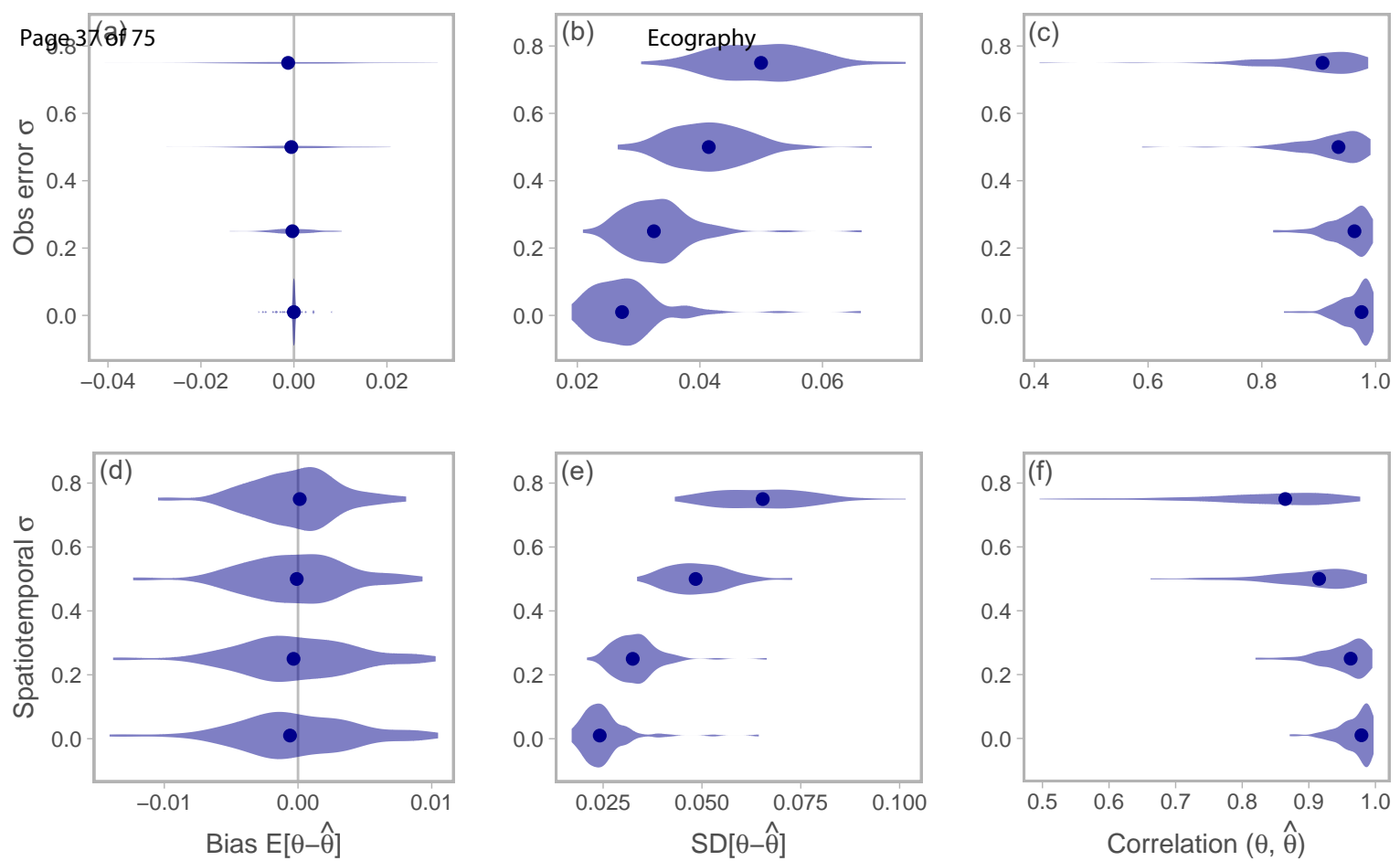
5

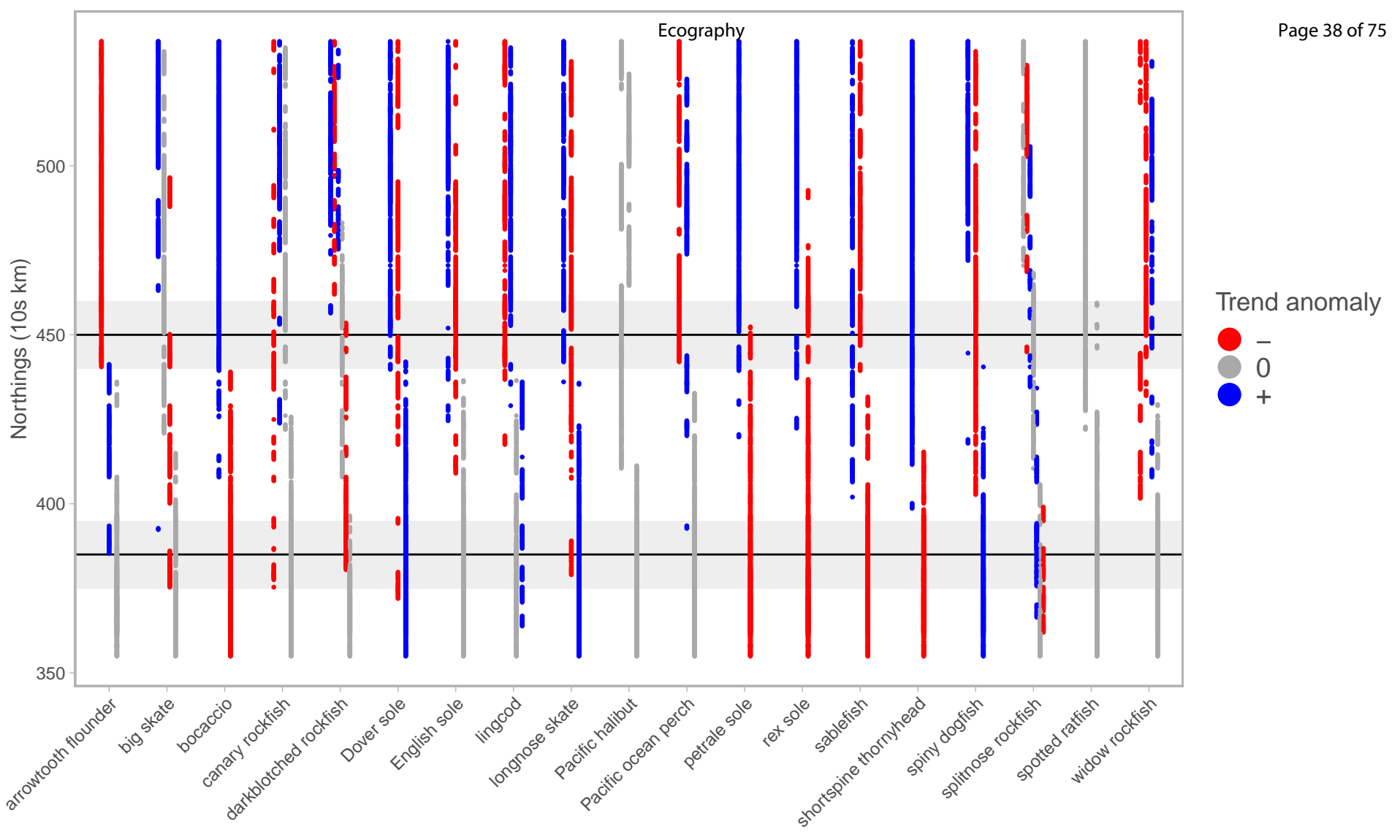


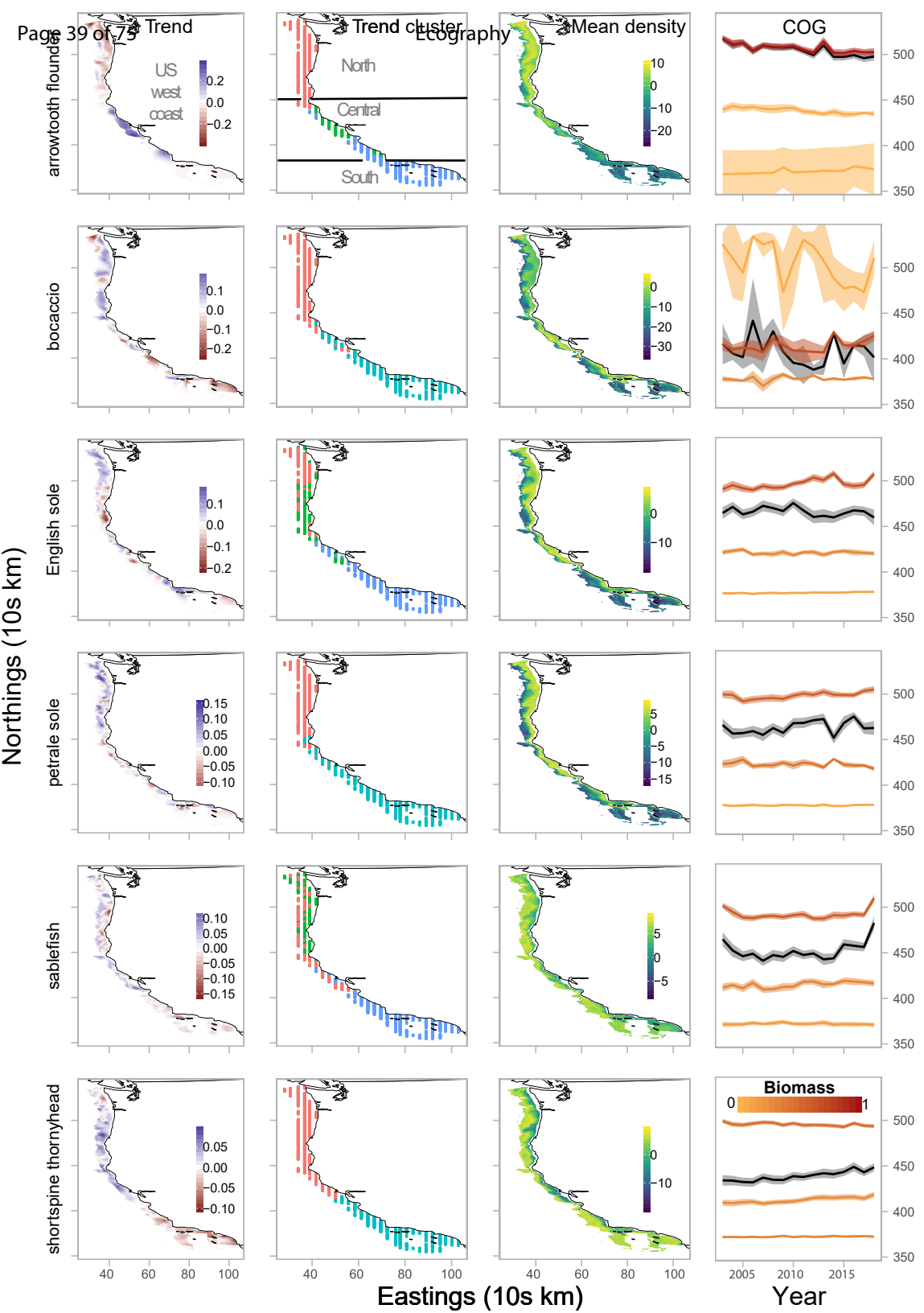
With spatially  
varying trend

Without spatially  
varying trend









1 APPENDIX 1: SUPPLEMENTARY METHODS, TABLES AND FIGURES

2

3 APPENDIX 1 SUPPLEMENTARY METHODS: SIMULATION OVERVIEW

4 For each combination of parameters (Table S1), we generated 100 simulated datasets.

5 First, we simulated random coordinates representing the locations of observed data (40 points,

6 uniform on a grid from 0-10 in the x- and y-axes). Using these knot locations we simulated data

7 from a spatial Matérn process using the `RandomFields::RFsimulate()` function in R. We chose to

8 simulate observations over a period of 10 years, and did not model any components of the model

9 as being autoregressive. We simulated observations with a Gaussian error distribution, and

10 assumed observation error to be constant over space and time. This simulated dataset includes a

11 spatial component (constant over time) and a spatiotemporal component (time varying, but

12 independent from year to year). To include a spatially explicit temporal trend (or local trend), we

13 used the same process as above, but for 1 time step (omitting the spatiotemporal component) and

14 fixing parameter values ( $\sigma_0$  shared with the spatial process of the observations – Table S1,  $\kappa_{trend}$

15 = 0.1). We then projected the effect of the local trend on the observations with a linear model

16 (e.g.,  $\hat{B}_0 = B_0 + B_1 t$ , but in 2-dimensions). All code to replicate these analyses are available on

17 GitHub: <https://github.com/fate-spatialindicators/spatial-trend>.

## 18 APPENDIX 1: TABLES

19 Table S1. Simulation parameters to evaluate sensitivity to spatiotemporal variation and  
 20 observation error.

Parameter	Interpretation	Value
T	Time steps	10
$\kappa$	Decay of spatial correlation	1
$\sigma_0$	Standard deviation of spatial process	0.01, 0.25, 0.5
$\sigma_E$	Standard deviation of spatiotemporal process	0.01, 0.25, 0.5, 0.75, 1
$\sigma_{obs\ error}$	Observation error scale	0.01, 0.25, 0.5, 0.75, 1
$\kappa_{trend}$	Decay of spatial correlation (local trend field)	0.1
$\sigma_{0,trend}$	Standard deviation of the spatial process (local trend field)	0.01, 0.25, 0.5

21  
 22 Table S2. Empirical occurrence and mean catch rates for positive tows (CPUE in kg/km<sup>2</sup>) for the  
 23 19 West Coast groundfish species included in our analysis.

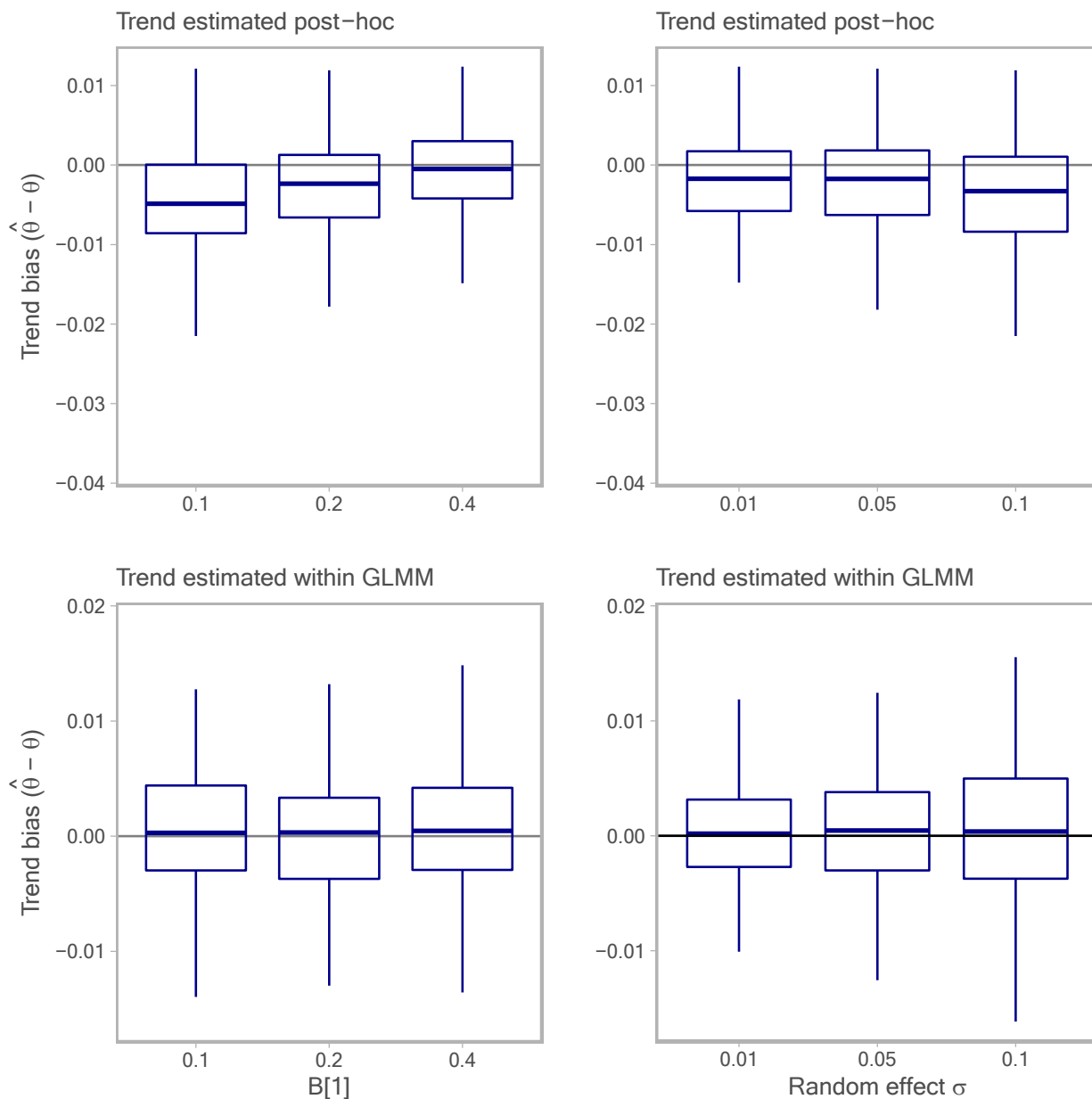
Species common name	Species	Occurrence	Mean CPUE
arrowtooth flounder	<i>Atheresthes stomias</i>	0.36	1535.47
big skate	<i>Raja binoculata</i>	0.15	826.21
bocaccio	<i>Sebastes paucispinis</i>	0.07	1116.80
canary rockfish	<i>Sebastes pinniger</i>	0.08	3217.57
darkblotched rockfish	<i>Sebastes crameri</i>	0.18	960.41
Dover sole	<i>Microstomus pacificus</i>	0.84	2968.49
English sole	<i>Parophrys vetulus</i>	0.41	695.70
lingcod	<i>Ophiodon elongatus</i>	0.33	873.42
longnose skate	<i>Raja rhina</i>	0.60	985.95
Pacific halibut	<i>Hippoglossus stenolepis</i>	0.08	1031.22
Pacific ocean perch	<i>Sebastes alutus</i>	0.07	2191.36
petrale sole	<i>Eopsetta jordani</i>	0.43	909.81
rex sole	<i>Glyptocephalus zachirus</i>	0.62	1011.33
sablefish	<i>Anoplopoma fimbria</i>	0.65	1191.93
shortspine thornyhead	<i>Sebastolobus alascanus</i>	0.51	690.99
North Pacific spiny dogfish	<i>Squalus suckleyi</i>	0.28	2819.21
splitnose rockfish	<i>Sebastes diploproa</i>	0.21	2619.62
spotted ratfish	<i>Hydrolagus colliei</i>	0.50	617.10
widow rockfish	<i>Sebastes entomelas</i>	0.04	1846.20

24 Table S3. Delta-AIC values comparing spatial GLMMs with and without an estimated spatial-  
25 trend field. Delta-AIC values are interpreted relative to the best model for each species (0 = most  
26 parsimonious model).

<i>Species common name</i>	<i>No local trend</i>	<i>Local trend</i>
arrowtooth flounder	87.10	<b>0.00</b>
big skate	<b>0.00</b>	0.81
bocaccio	6.25	<b>0.00</b>
canary rockfish	4.55	<b>0.00</b>
darkblotched rockfish	6.30	<b>0.00</b>
Dover sole	88.24	<b>0.00</b>
English sole	45.79	<b>0.00</b>
lingcod	3.43	<b>0.00</b>
longnose skate	28.43	<b>0.00</b>
Pacific halibut	<b>0.00</b>	1.90
Pacific ocean perch	0.67	<b>0.00</b>
petrale sole	25.87	<b>0.00</b>
rex sole	88.61	<b>0.00</b>
sablefish	20.23	<b>0.00</b>
shortspine thornyhead	35.38	<b>0.00</b>
North Pacific spiny dogfish	38.58	<b>0.00</b>
splitnose rockfish	1.28	<b>0.00</b>
spotted ratfish	15.83	<b>0.00</b>
widow rockfish	5.60	<b>0.00</b>

27

## 28 APPENDIX 1: FIGURES

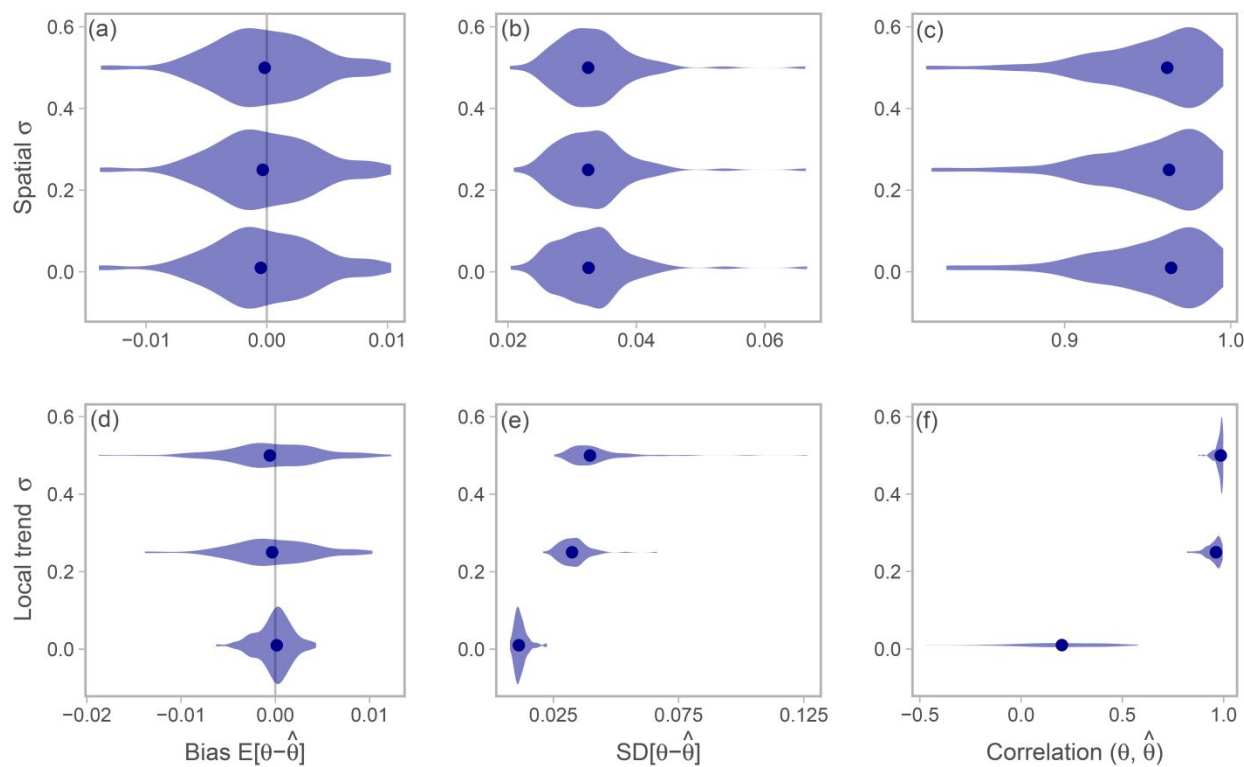


29

30 Fig. S1. Estimates of linear trend in a generalized linear mixed model. Plots are based on 1000  
 31 simulated data sets, 15 time steps each, with multiple observations ( $n=2$ ) every other time step.  
 32 The underlying model included both a linear trend (with magnitude  $B[1]$ ) and varying degrees of  
 33 inter-annual variability (with magnitude determined by the random effect  $\sigma$ , the standard  
 34 deviation of the temporal random effects). Two estimation models were fit to each of the 1000

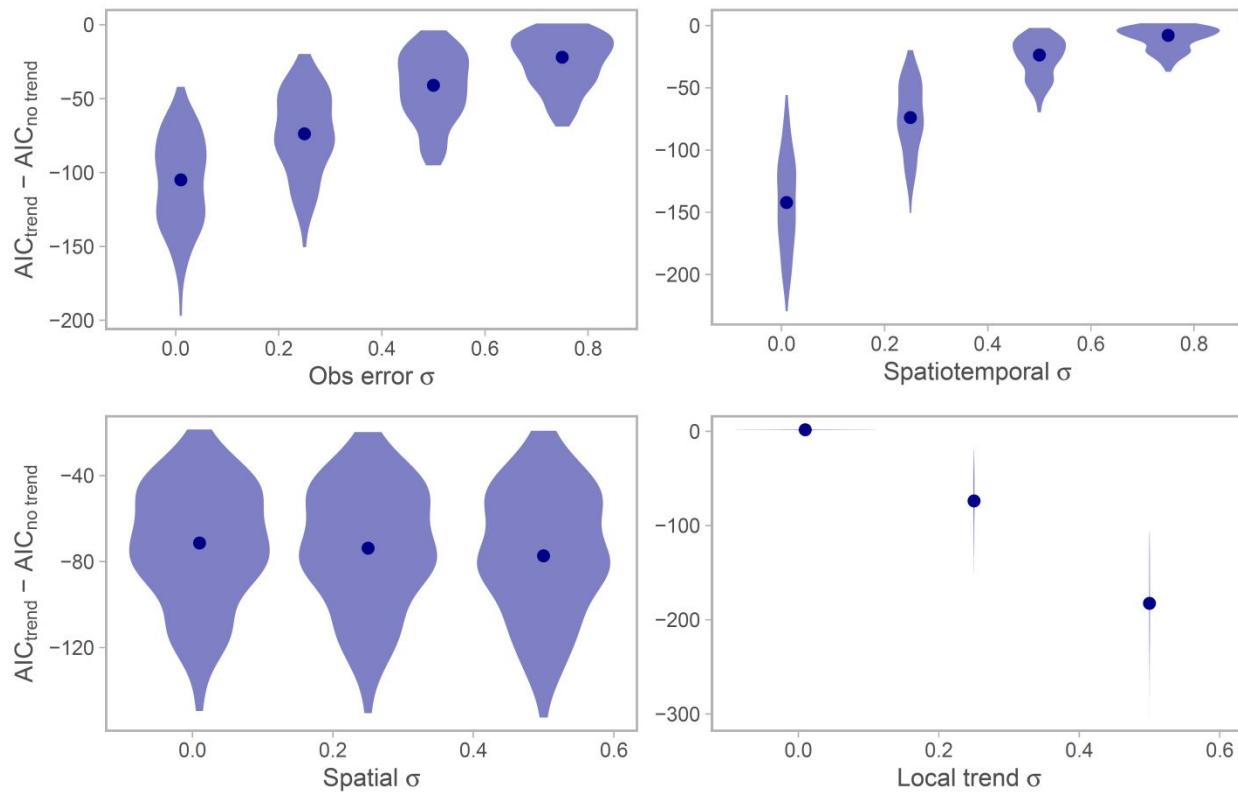
35 datasets: (1) a GLMM that included random effects, but not an explicit trend ('Trend estimated  
 36 post-hoc') and (2) a GLMM that included both random effects and linear trend. For the post-hoc  
 37 model, a trend estimate was generated by regressing time against the estimated temporal random  
 38 effects. For both models, we calculated the bias of the trend estimated versus the known value.

39



40

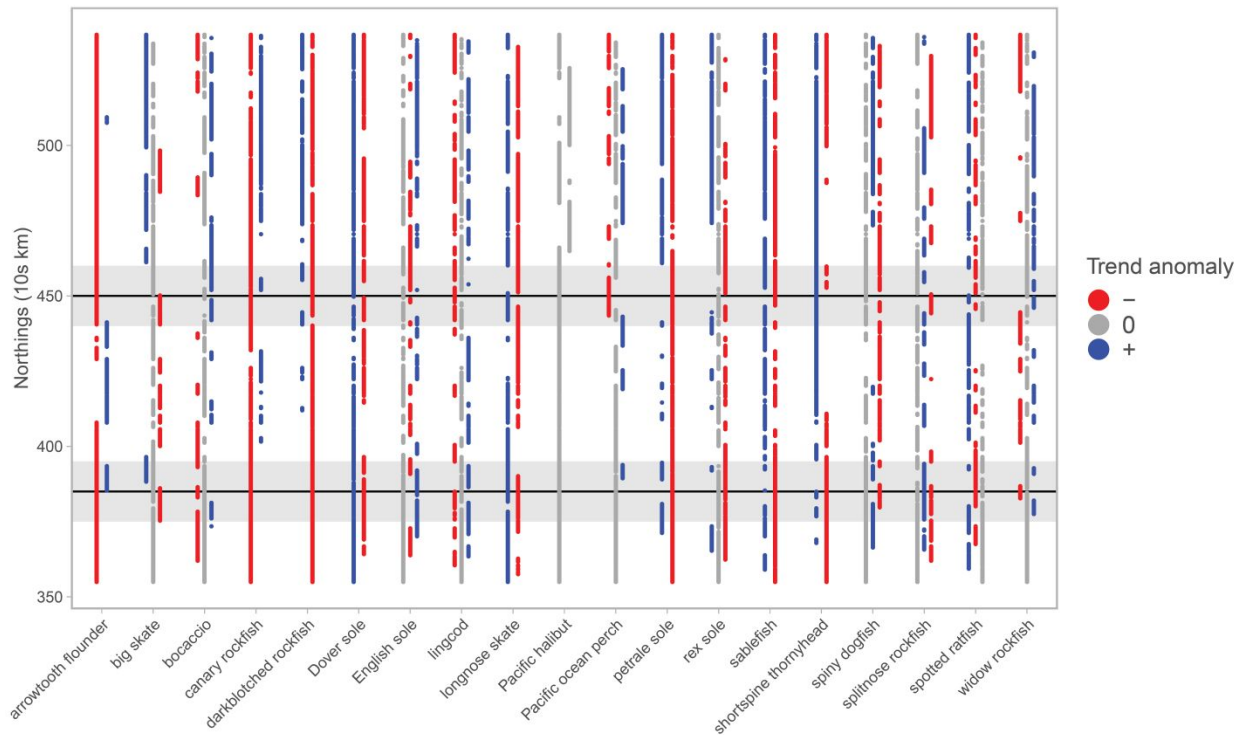
41 Fig. S2. Simulation testing the effects of spatial variation and local trend variation on the ability  
 42 to recover the local trend. The symbols  $\theta$  and  $\hat{\theta}$  refer to the local trend random effect values at  
 43 each location  $\mathbf{z}_s$  and their estimate, respectively. Each violin represents the distribution of  
 44 location by location comparisons from 100 simulations and the dots represent the median value.  
 45 In all cases, the standard deviation of the non-varying parameter is held at 0.01, while  $\sigma$  varies  
 46 along  $\{0.01, 0.25, 0.5\}$ .



47

48 Fig. S3. Simulation testing the effects of variation in observation error and the spatial,  
 49 spatiotemporal and local trend fields on the ability to identify the correct model structure using  
 50 information criterion. Each violin represents the distribution of the difference in AIC between a  
 51 GLMMs with and without the local trend from 100 simulations, and the dots represent the  
 52 median value. In all cases, the standard deviation of the non-varying parameter is held at 0.01,  
 53 while  $\sigma$  varies along  $\{0.01, 0.25, 0.5\}$  in addition to 0.75 for the observation error and  
 54 spatiotemporal  $\sigma$ .

55



56

57 Fig. S4. Strip plot showing each unique local trend (slope over time) cluster by species. This is  
 58 the same as Figure 4 of the main text, but without clustering simultaneously on latitude (and here  
 59 showing results from a search over a limited number of clusters to ease comparison of patterns in  
 60 cluster breaks between this figure and Figure 4 of the main text). Each set of points associated  
 61 with a given cluster are represented by a different column and colored by their deviation from the  
 62 mean coast-wide trend for a given species. Grey points represent clusters from which the trend  
 63 was within 0.01 of the mean coast-wide trend. Horizontal black lines represent approximate  
 64 positions of known biogeographic breaks: Cape Mendocino, California, in the north; Point  
 65 Conception, California, in the south. Horizontal gray shading represents a buffer of 100km  
 66 around each biogeographic boundary, which provide a benchmark for the proximity statistics  
 67 described in the main text.

68

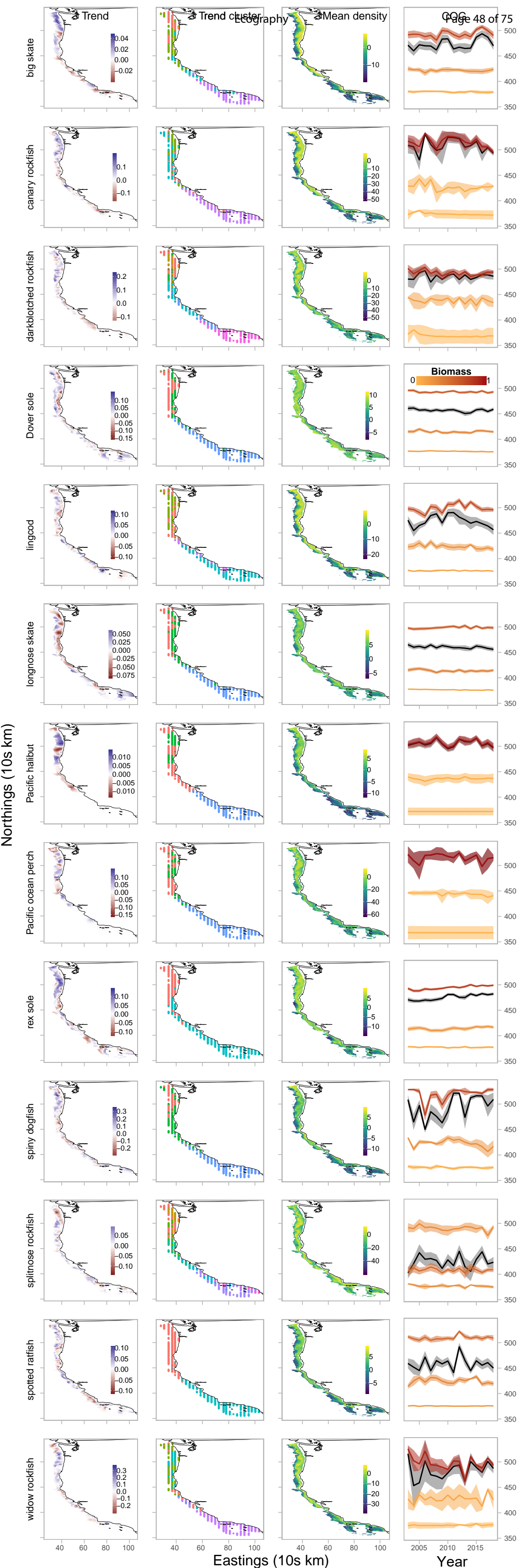
69 Fig. S5. Spatial and temporal patterns of predicted density for additional species not shown in  
70 Figure 5 of the main text. The first column shows maps of the predicted local trend (slope of log  
71 density across years). The second shows how each spatial location groups with a unique cluster  
72 of latitude and local trend. The third column represents the mean density over all years (in units  
73 of kg/km<sup>2</sup> on a log scale). The fourth column shows the time series of the center of gravity  
74 (COG), or latitude weighted by density, with 95% confidence intervals. The black line with grey  
75 interval represents the COG calculated from predicted densities coastwide, whereas the colored  
76 lines represent the COGs for each unique biogeographic region (separated by Cape Mendocino,  
77 California, in the north; Point Conception, California, in the south). Line color represents the  
78 proportion of a species' relative biomass in a given region. Note that for Pacific Ocean perch, the  
79 coastwide COG time series is completely overlapped by the northern regional COG.

80 [Figure attached as PDF]

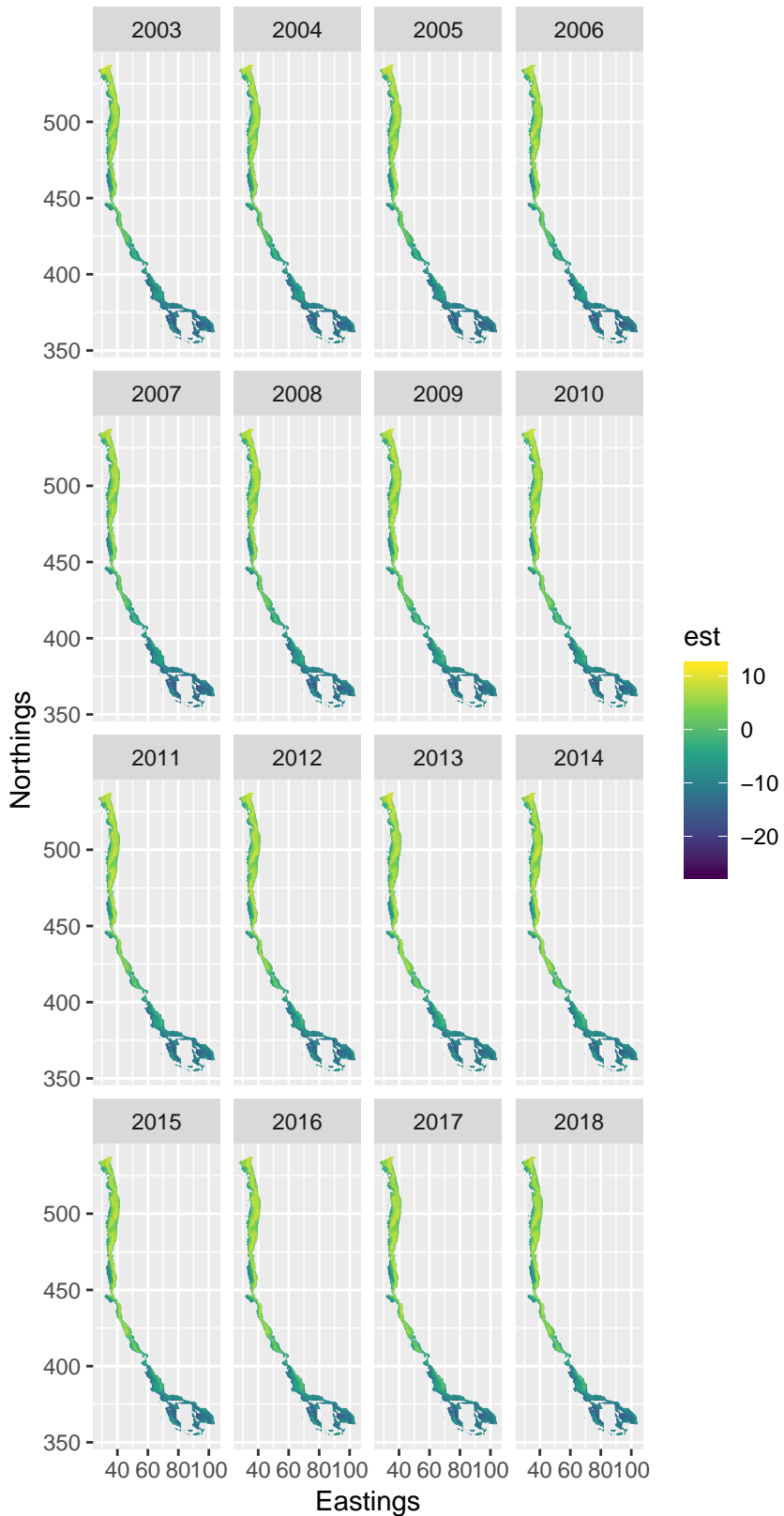
81

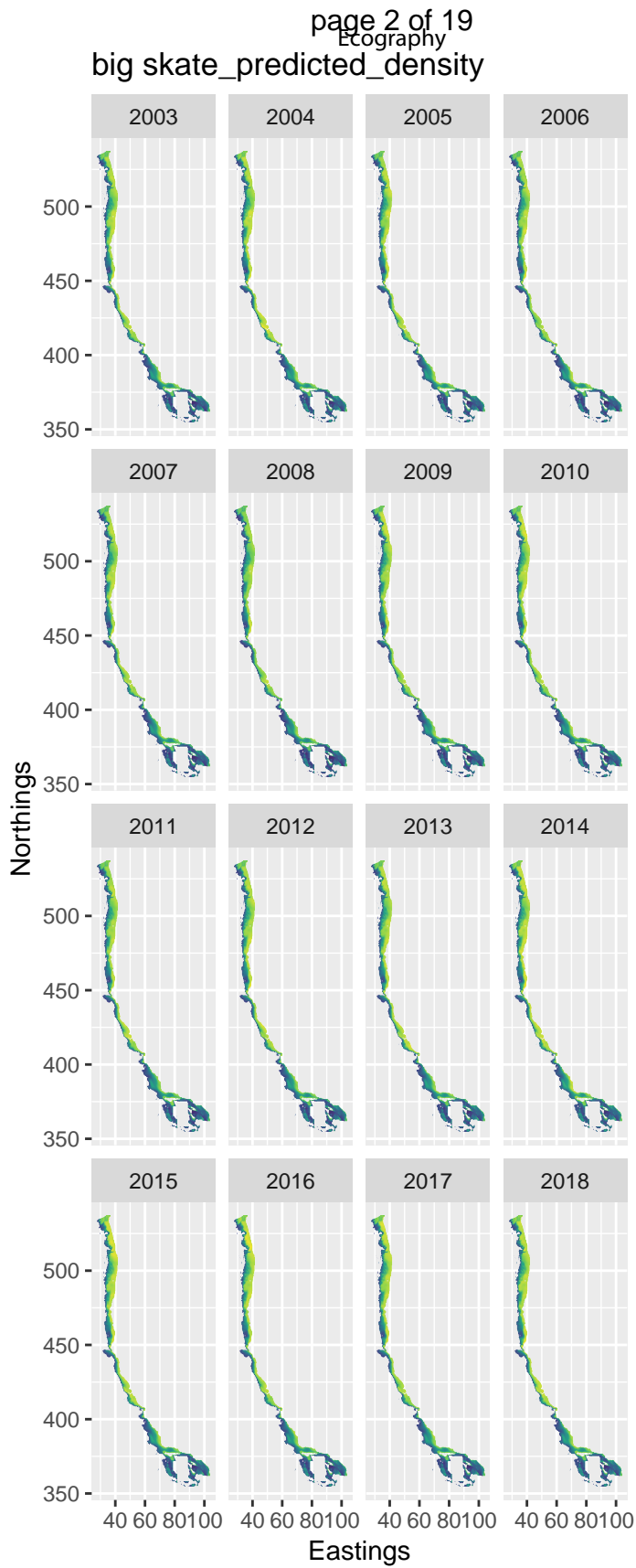
82 Fig. S6. Predicted density maps for the full study region by year for all species (in units of  
83 kg/km<sup>2</sup> on a log scale). Note that coordinates are scaled to 10s of km.

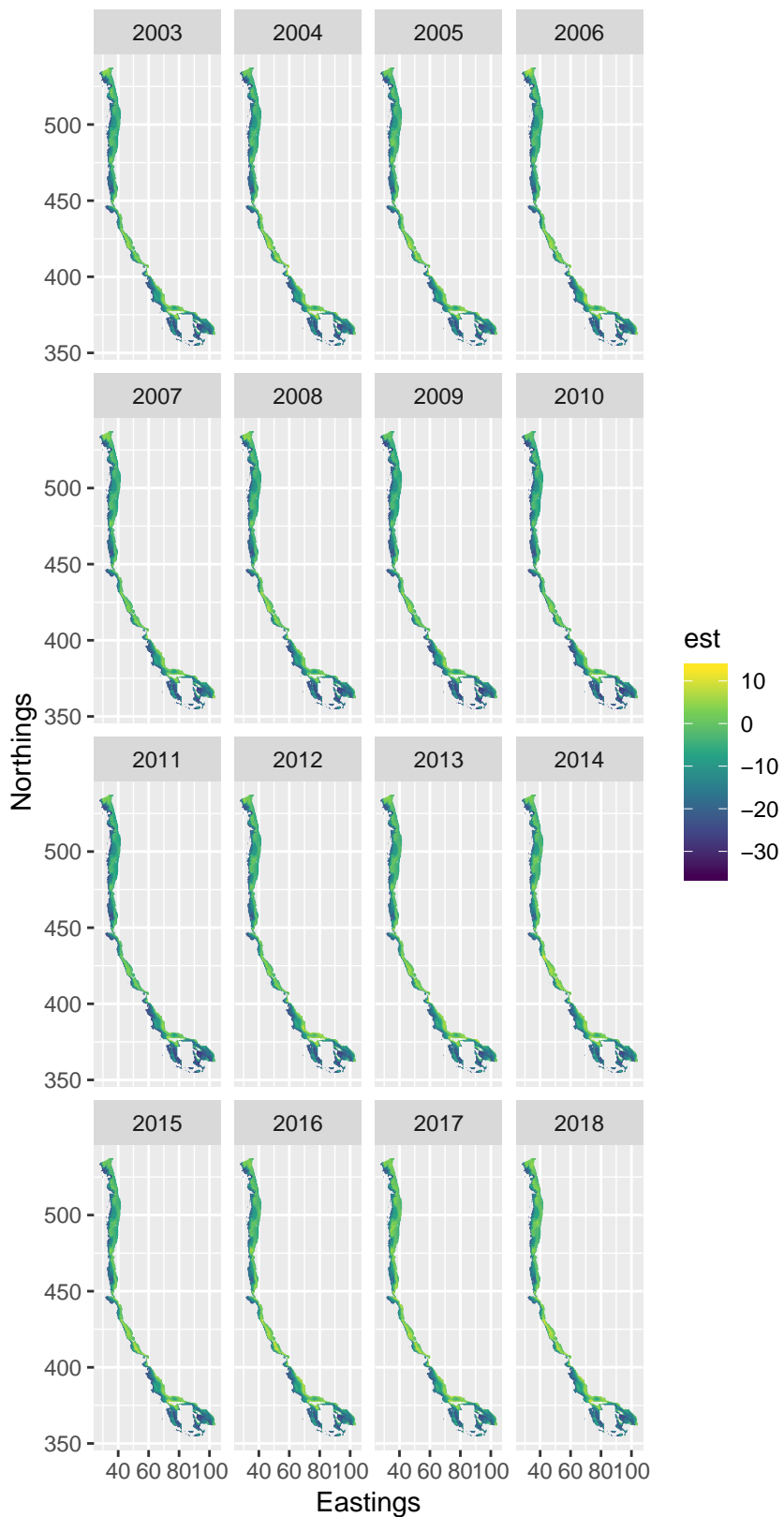
84 [Figure attached as PDF]



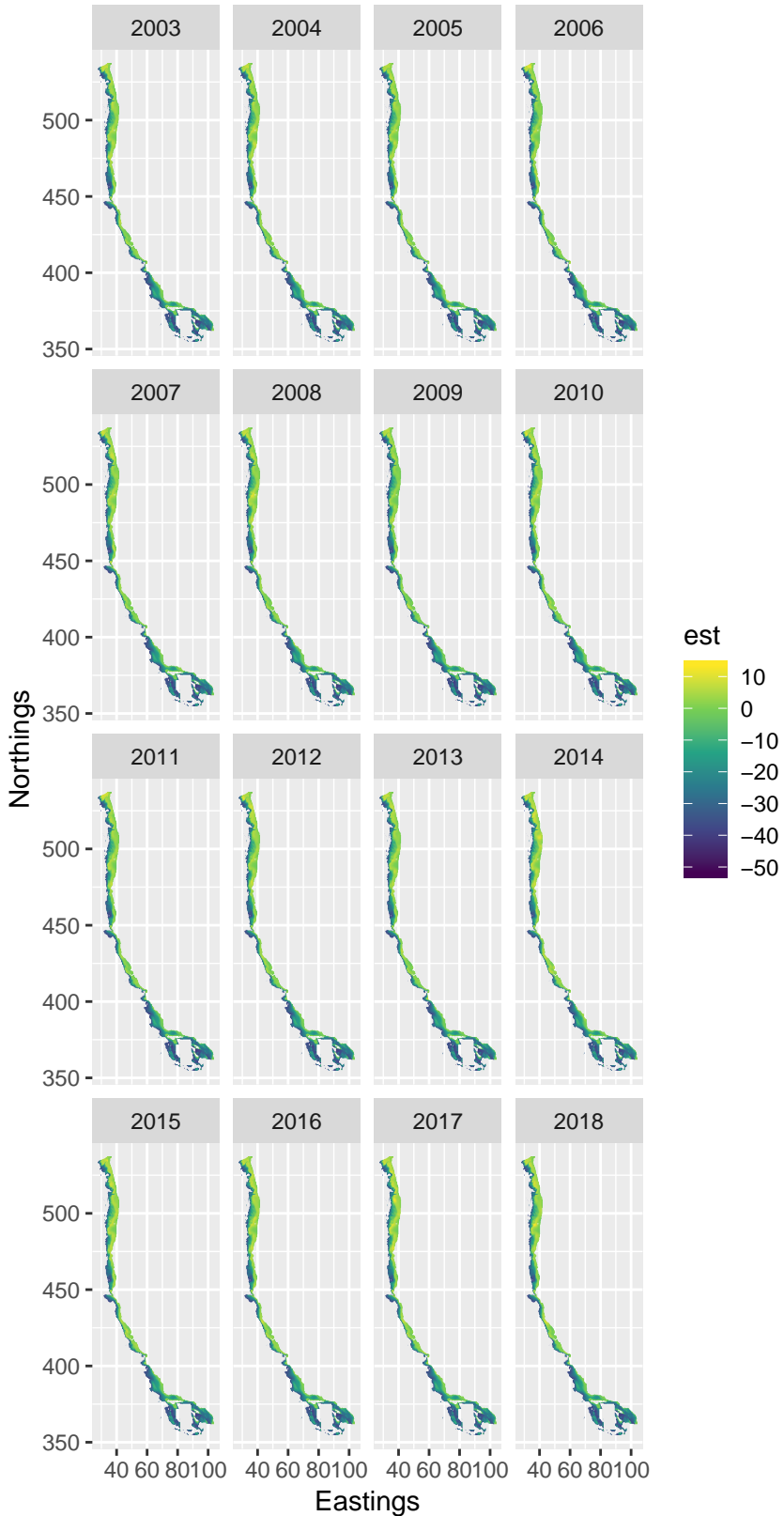
## arrowtooth flounder\_predicted\_density



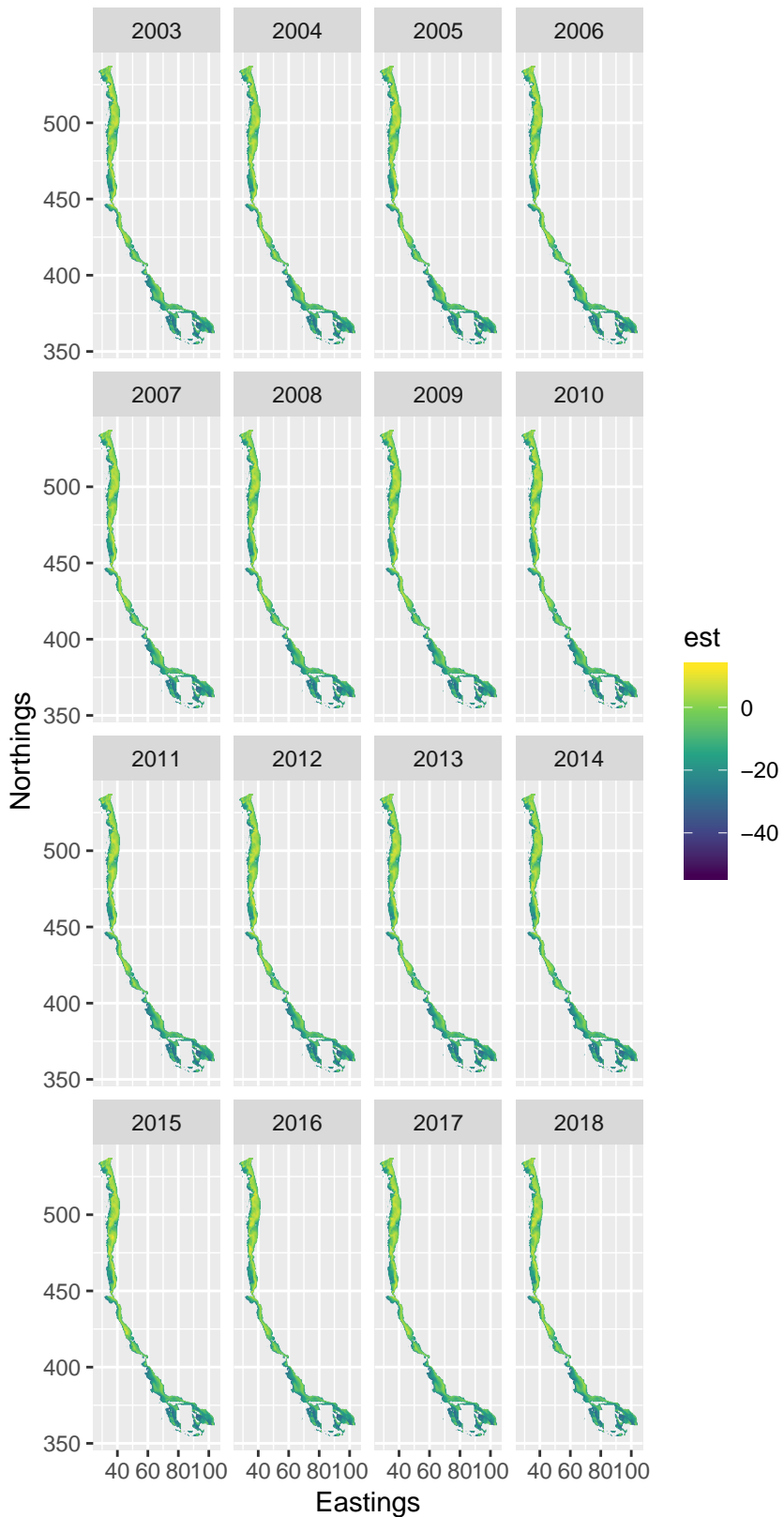




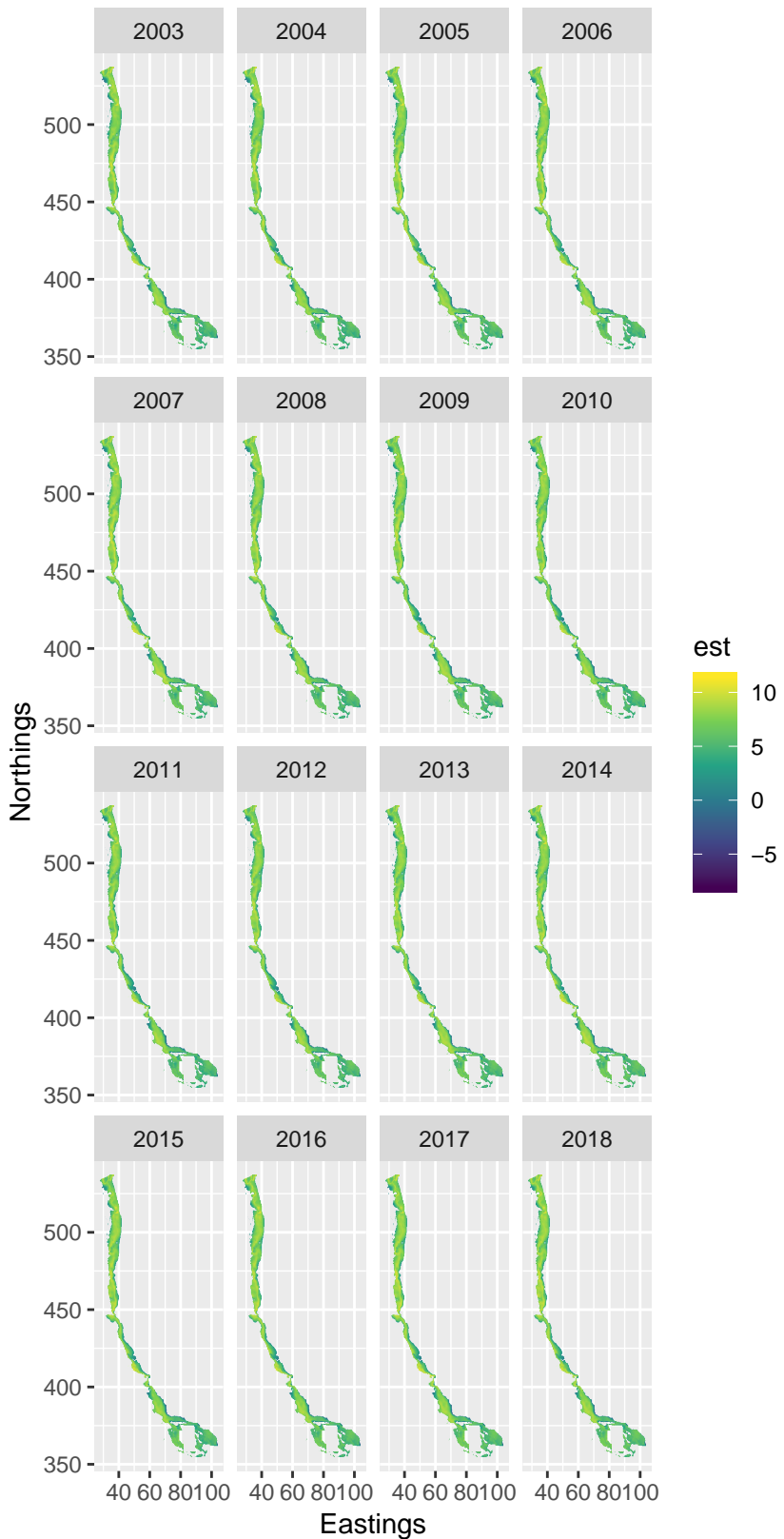
## canary rockfish\_predicted\_density



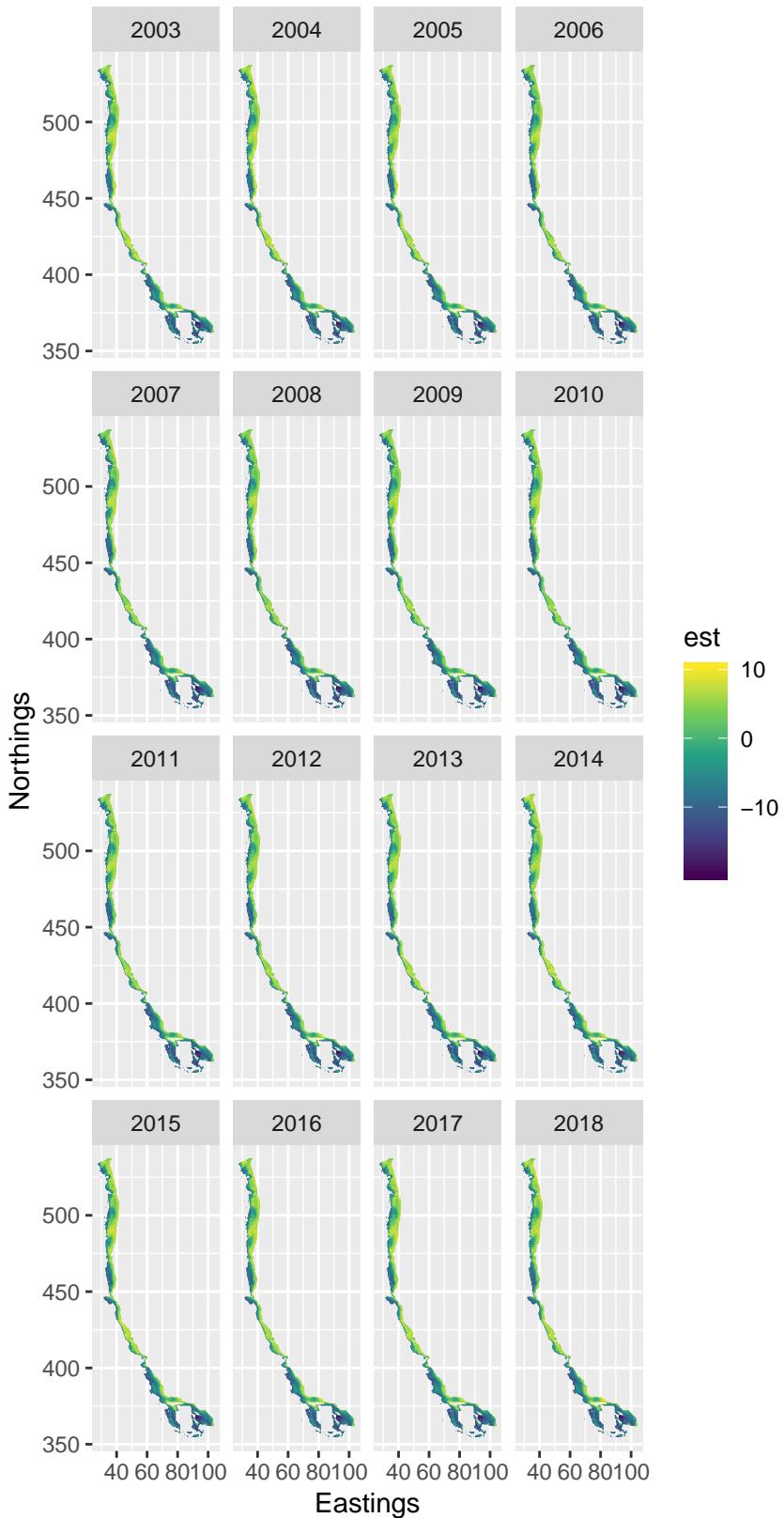
## darkblotched rockfish\_predicted\_density

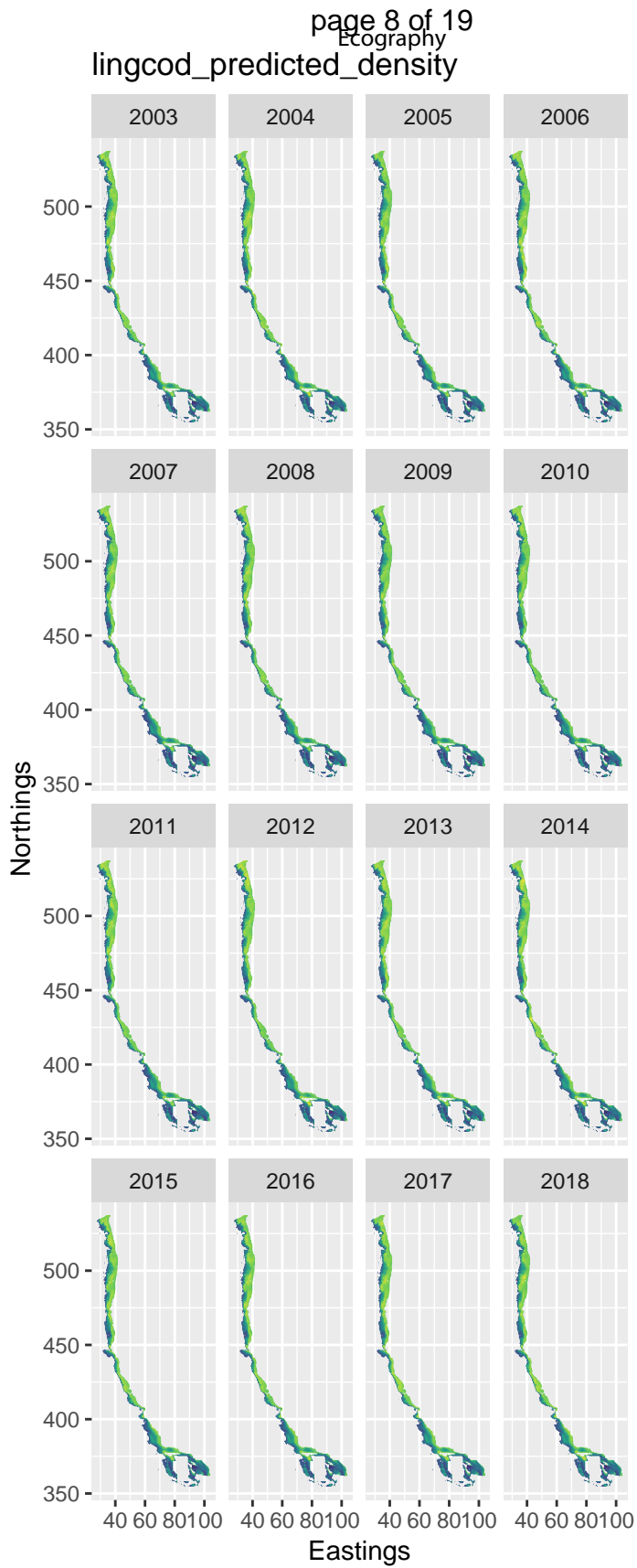


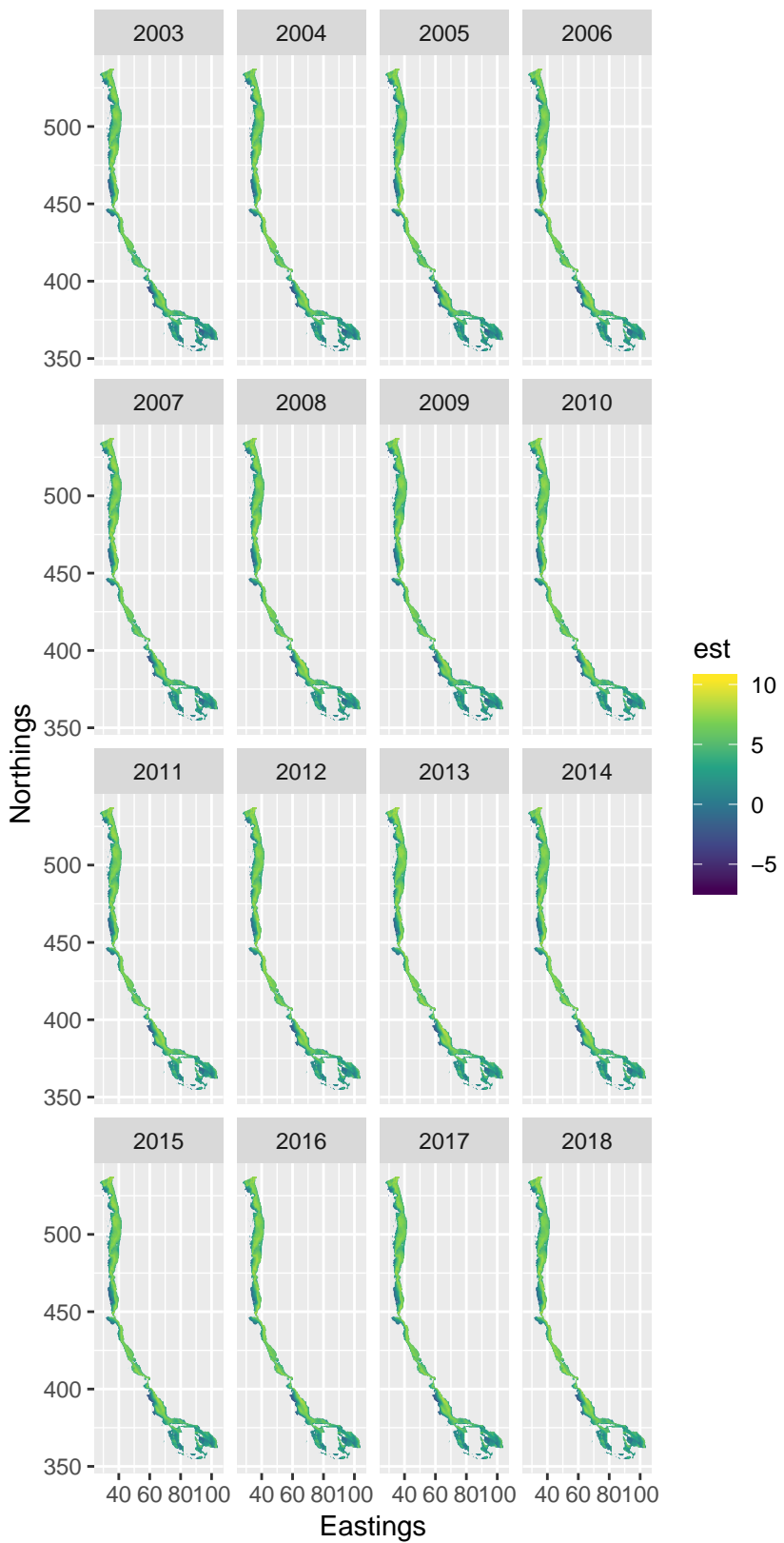
## Dover sole\_predicted\_density



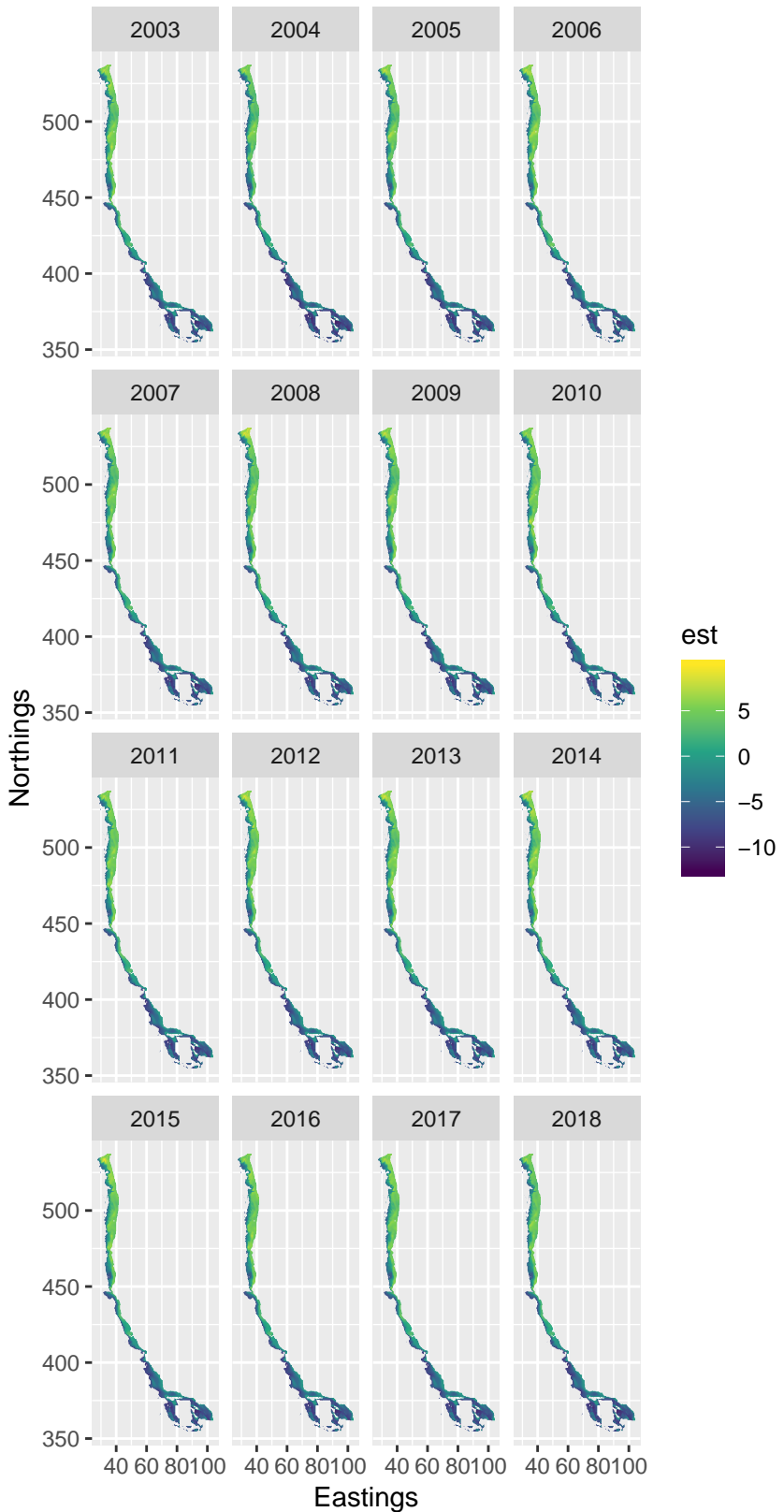
## English sole\_predicted\_density

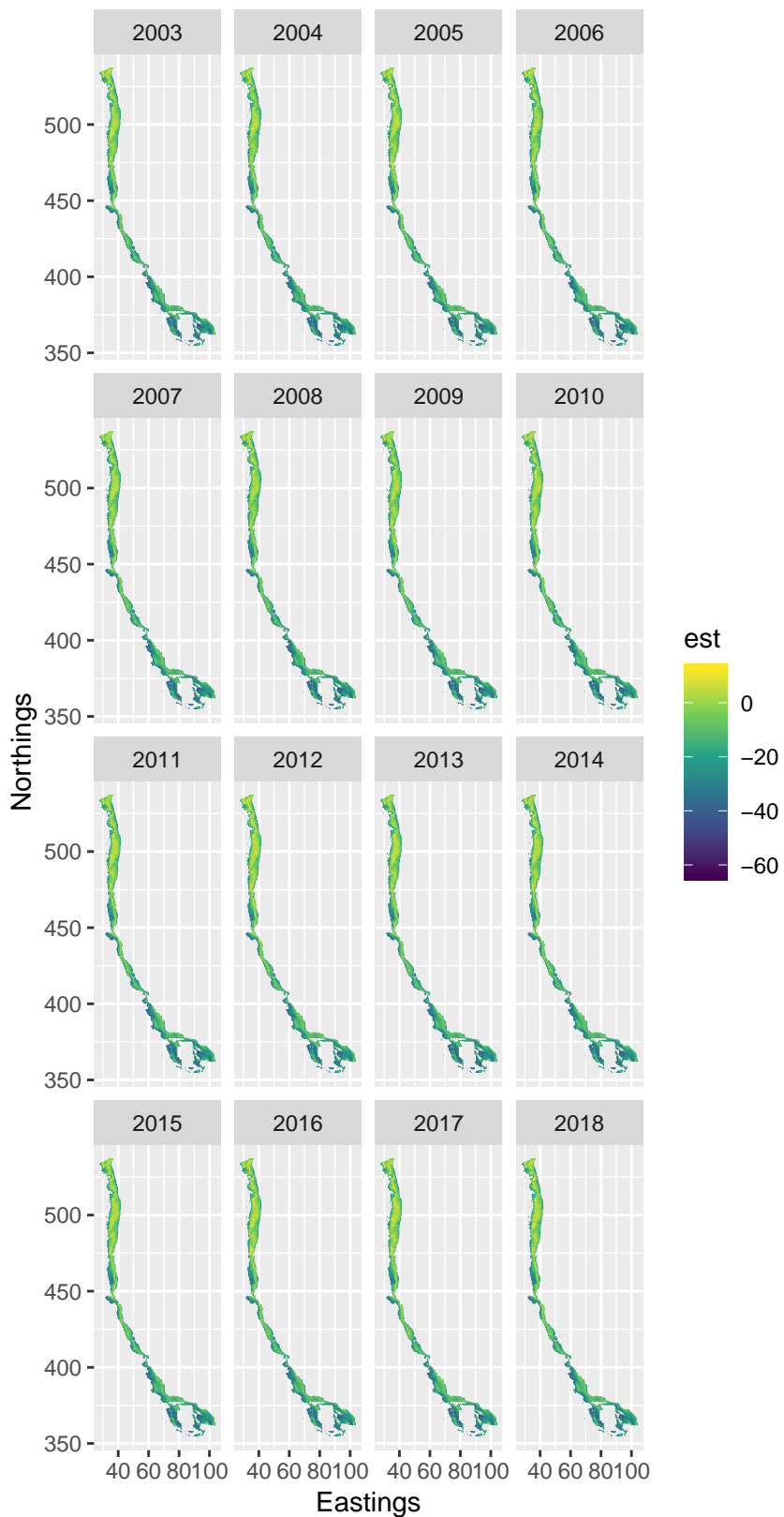


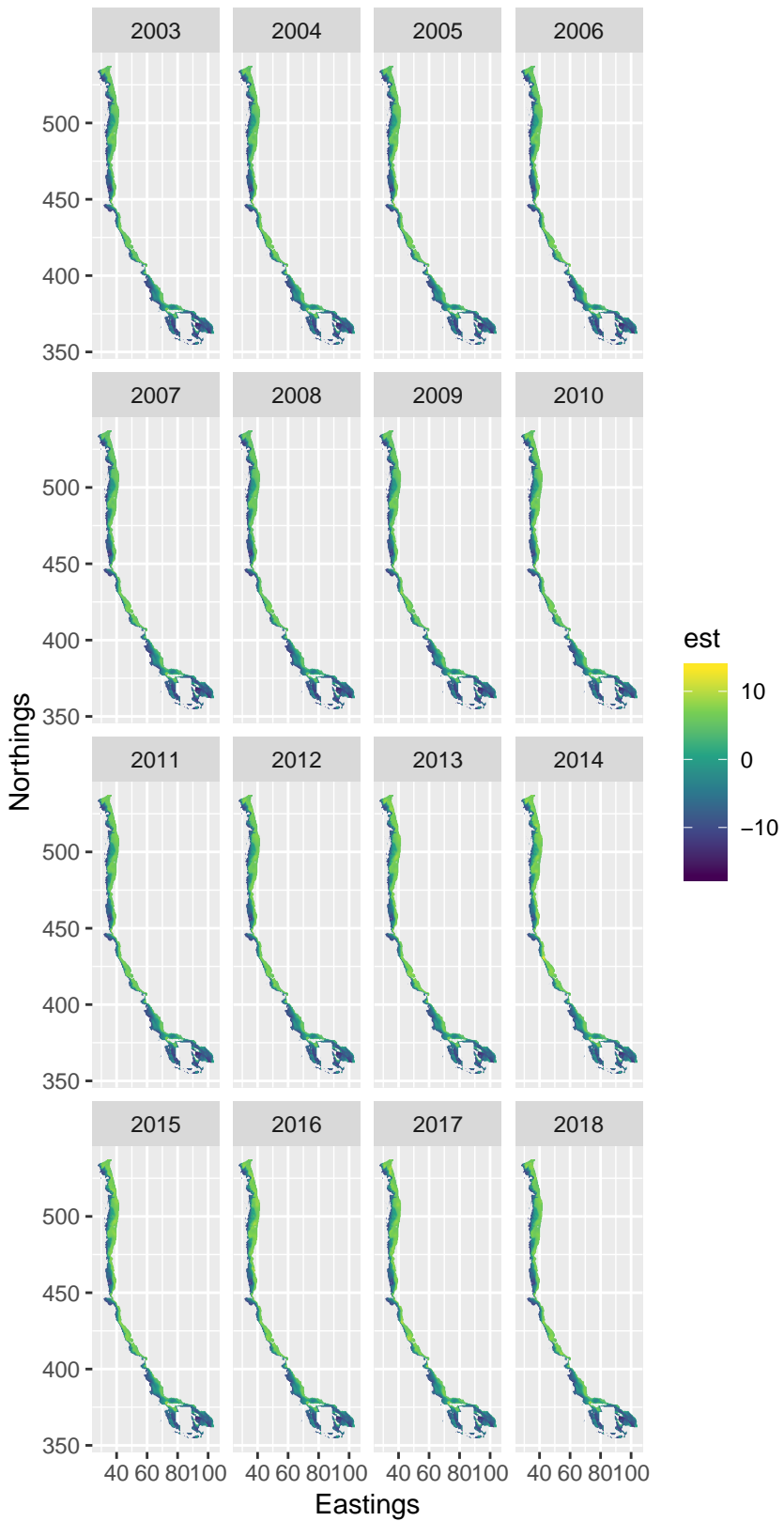


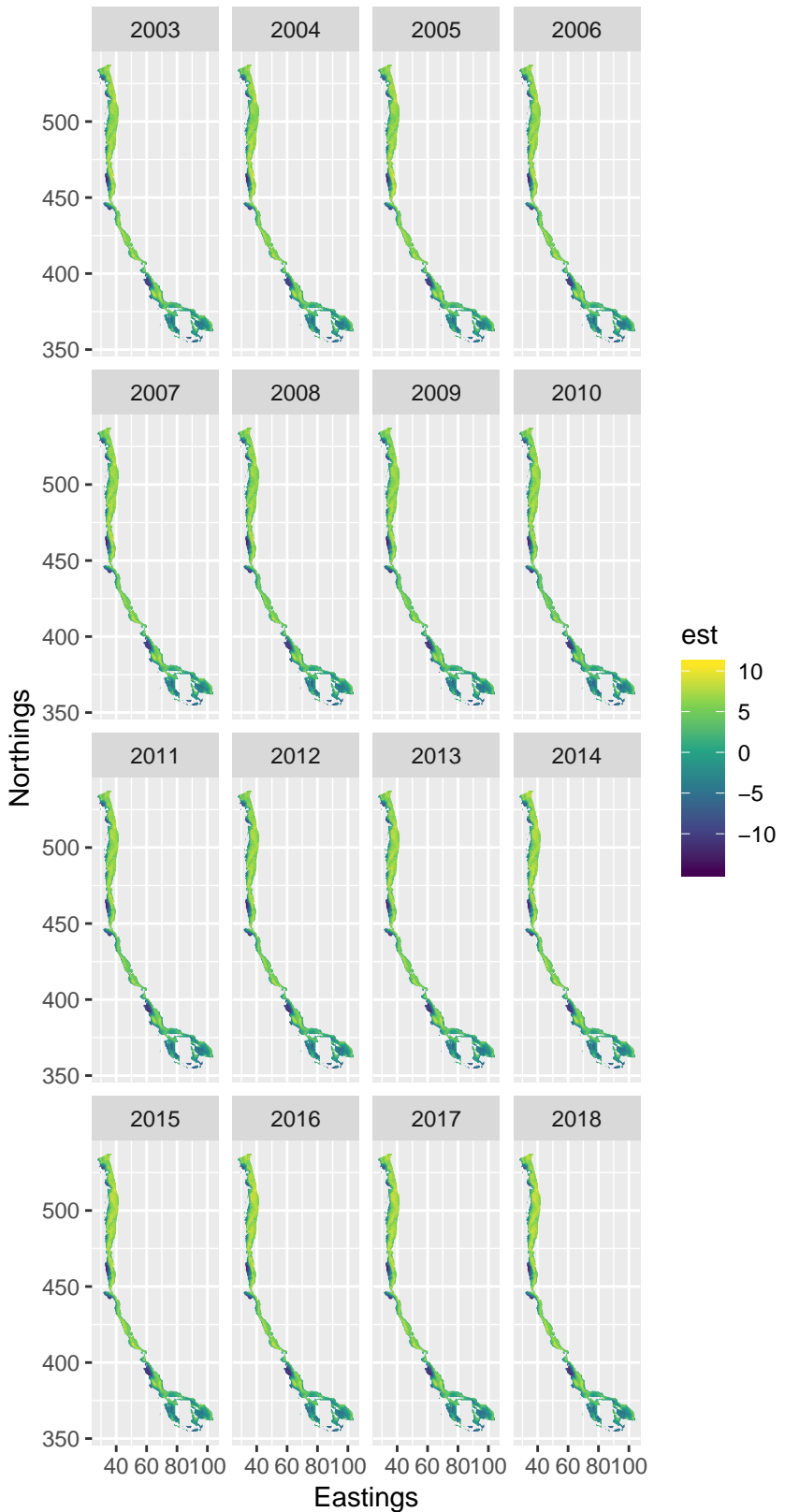
page 9 of 19  
Ecography  
longnose skate\_predicted\_density

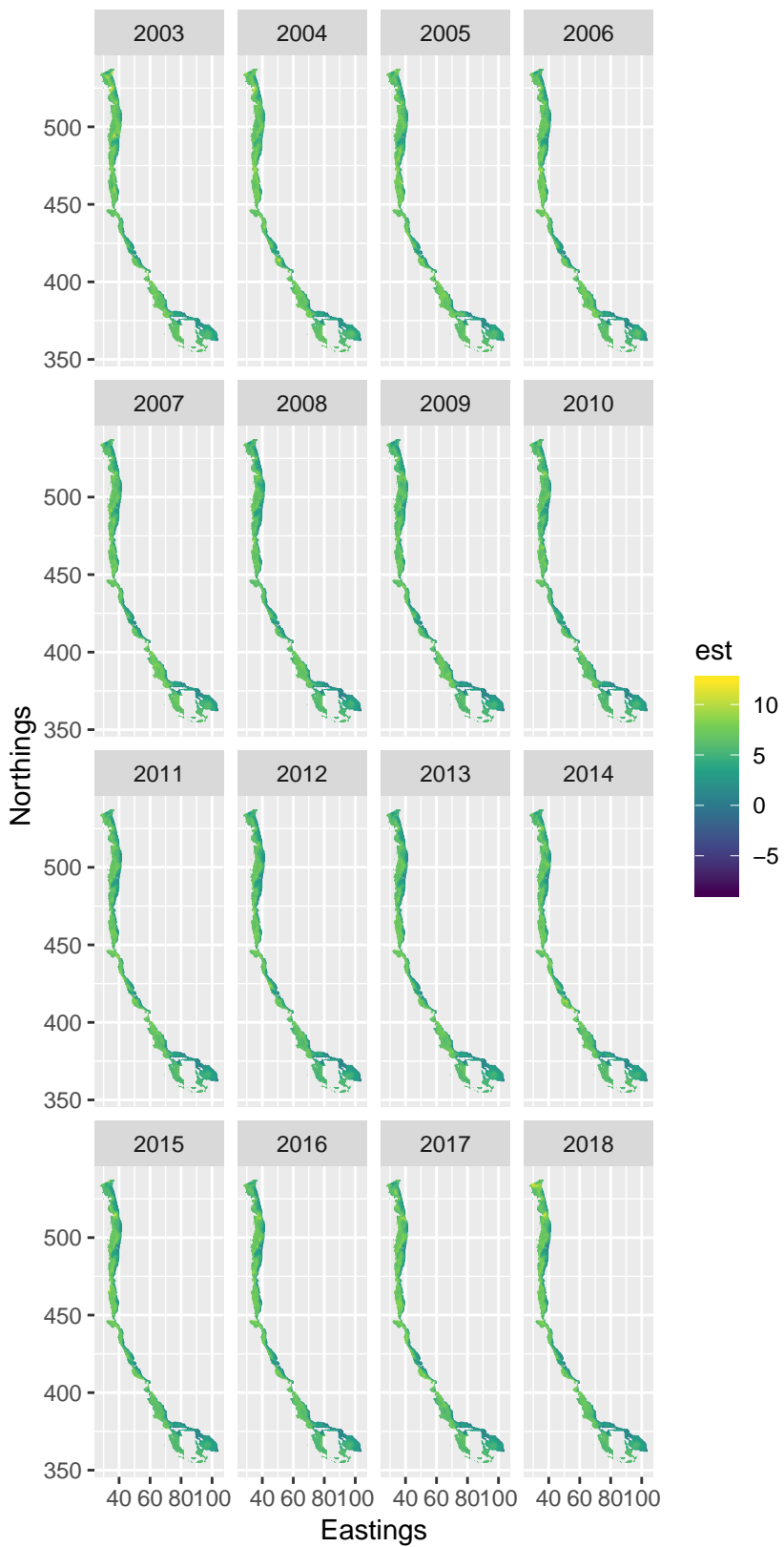
## Pacific halibut\_predicted\_density

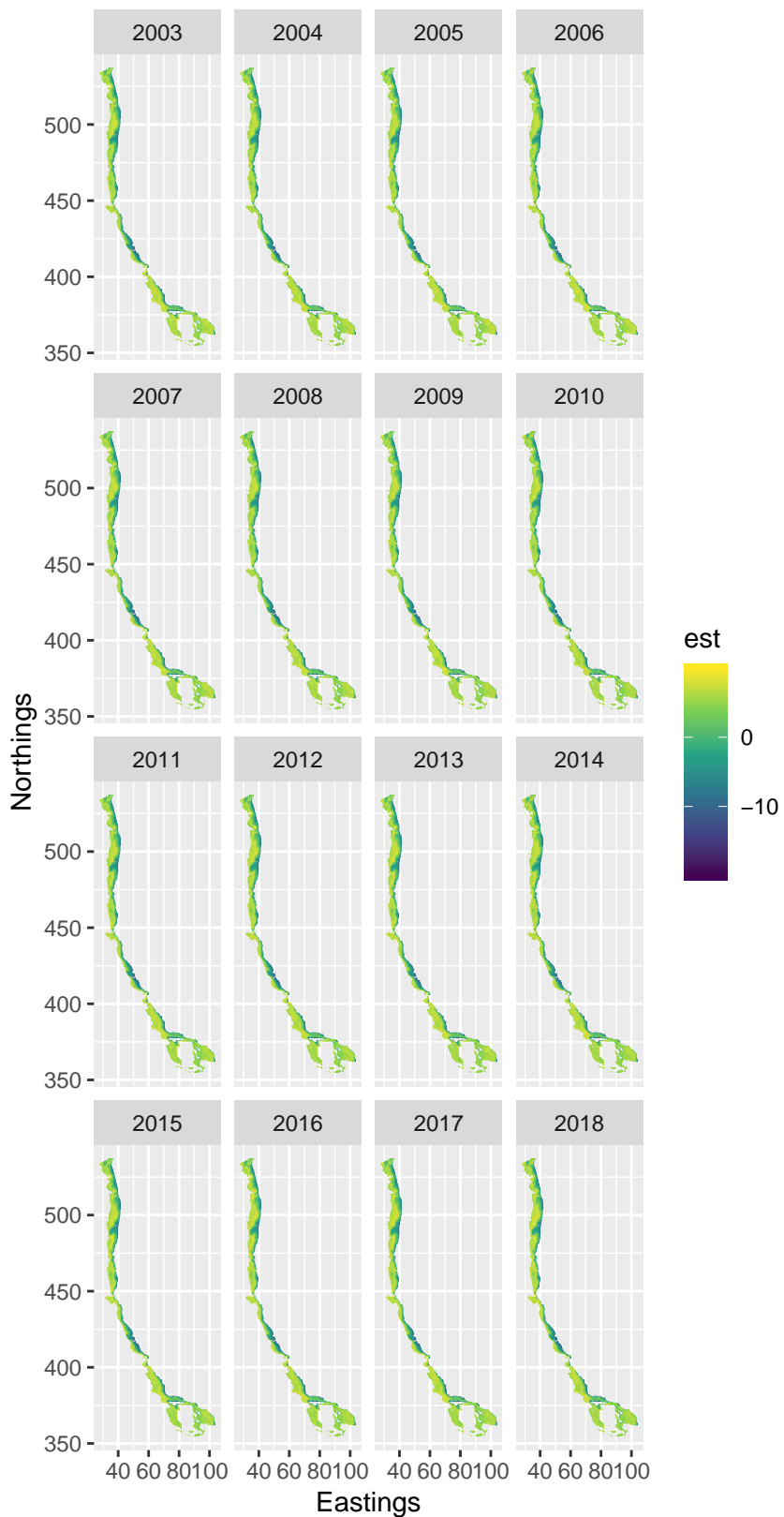


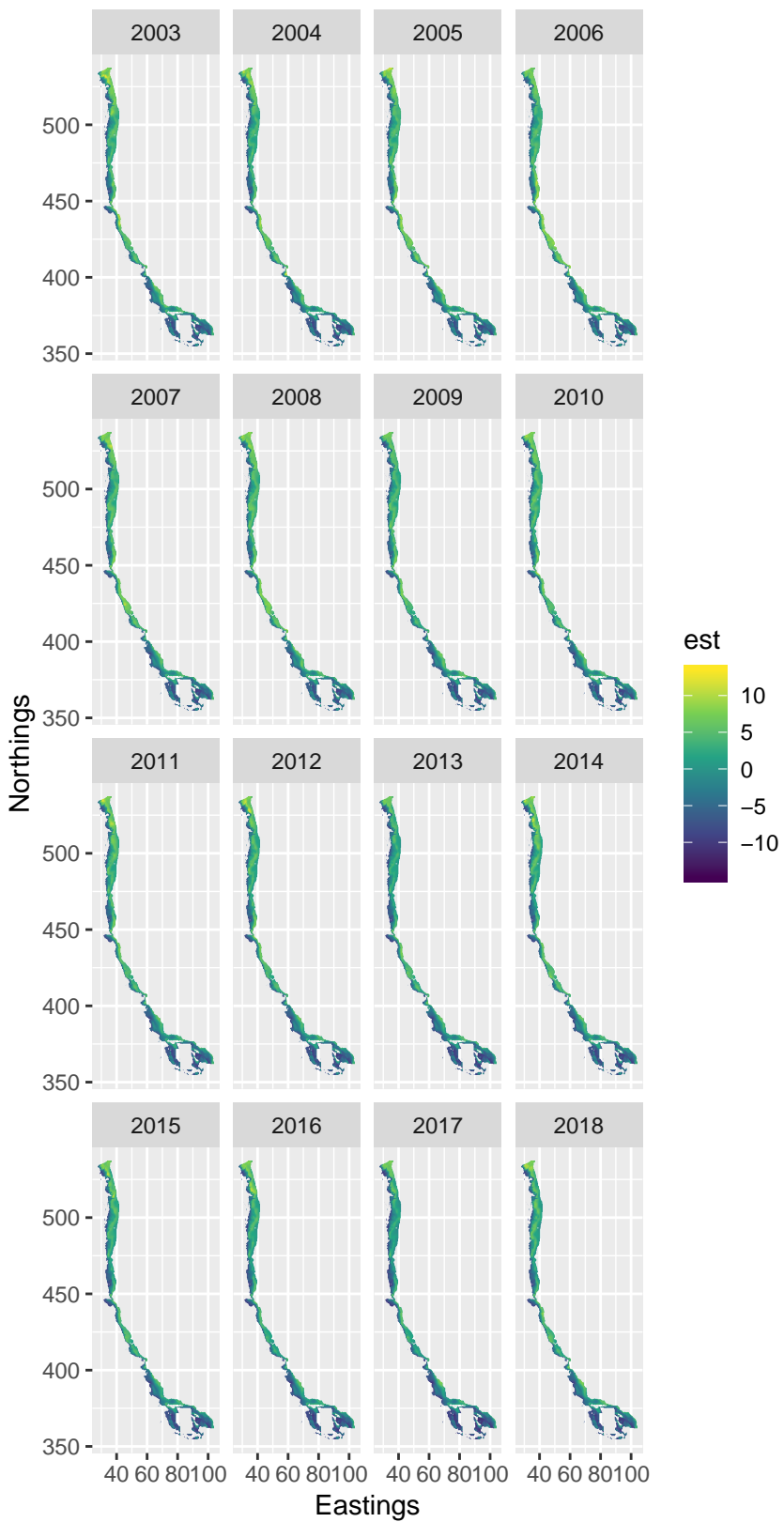
page 11 of 19  
Ecography  
Pacific ocean perch\_predicted\_density

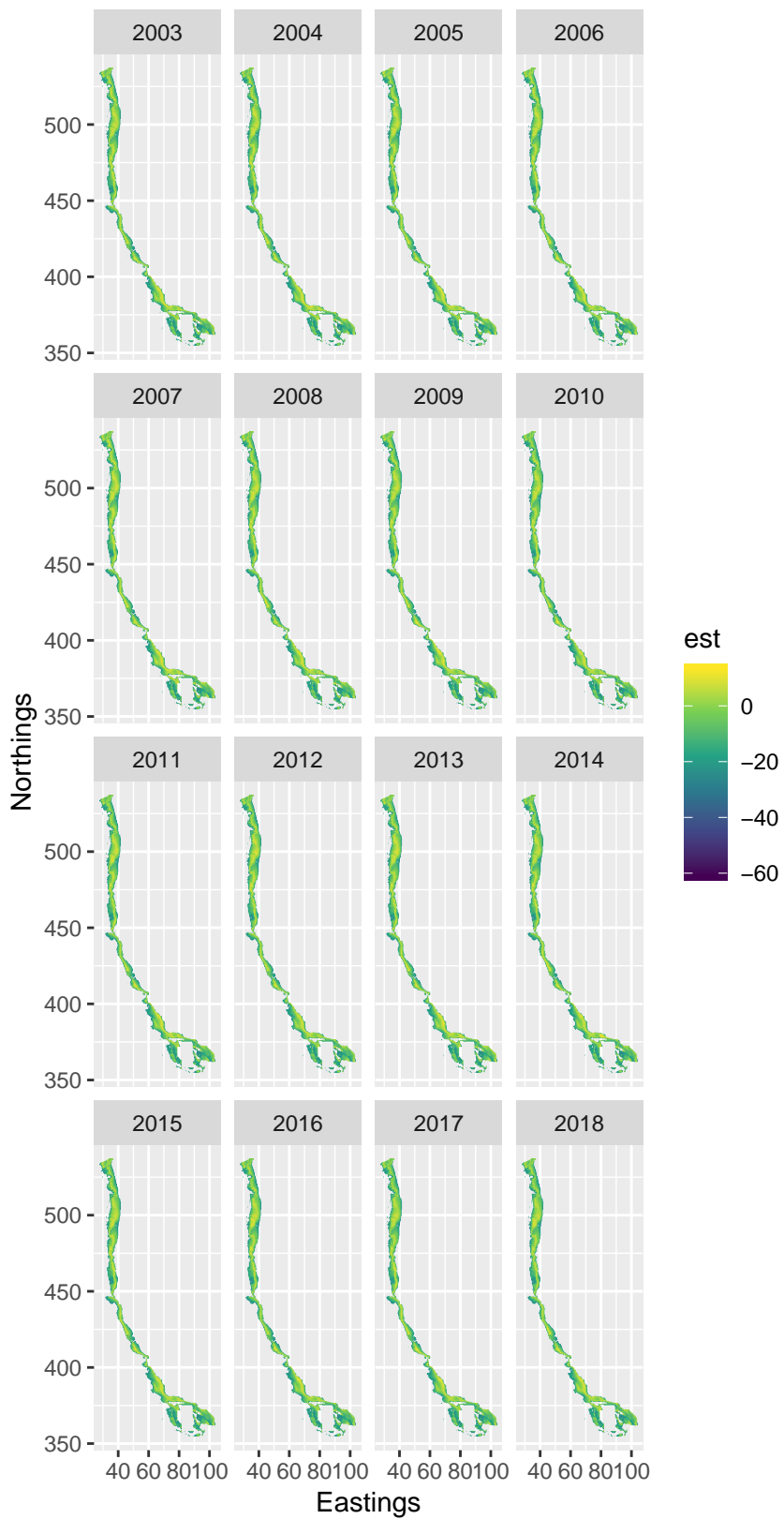


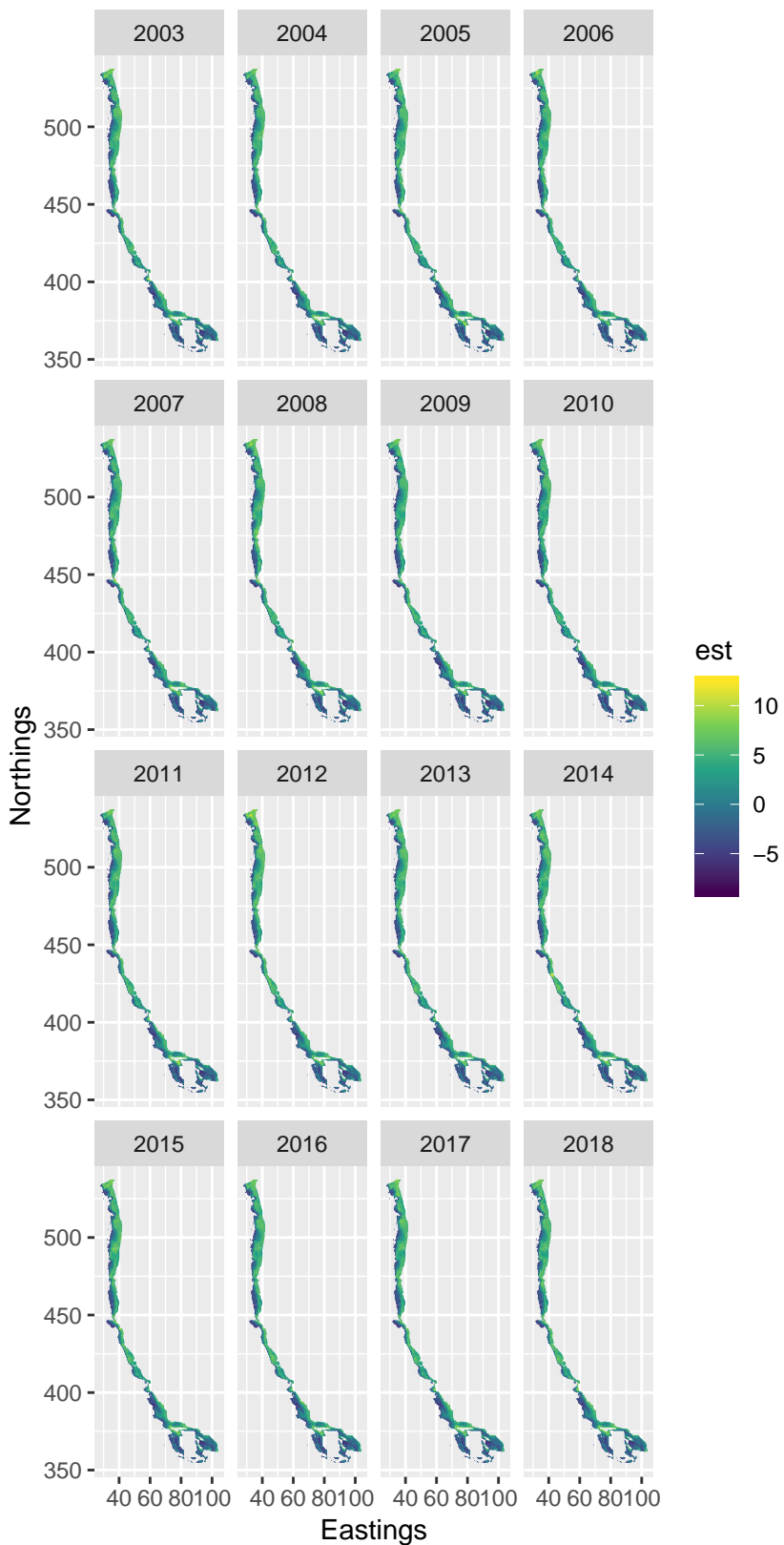


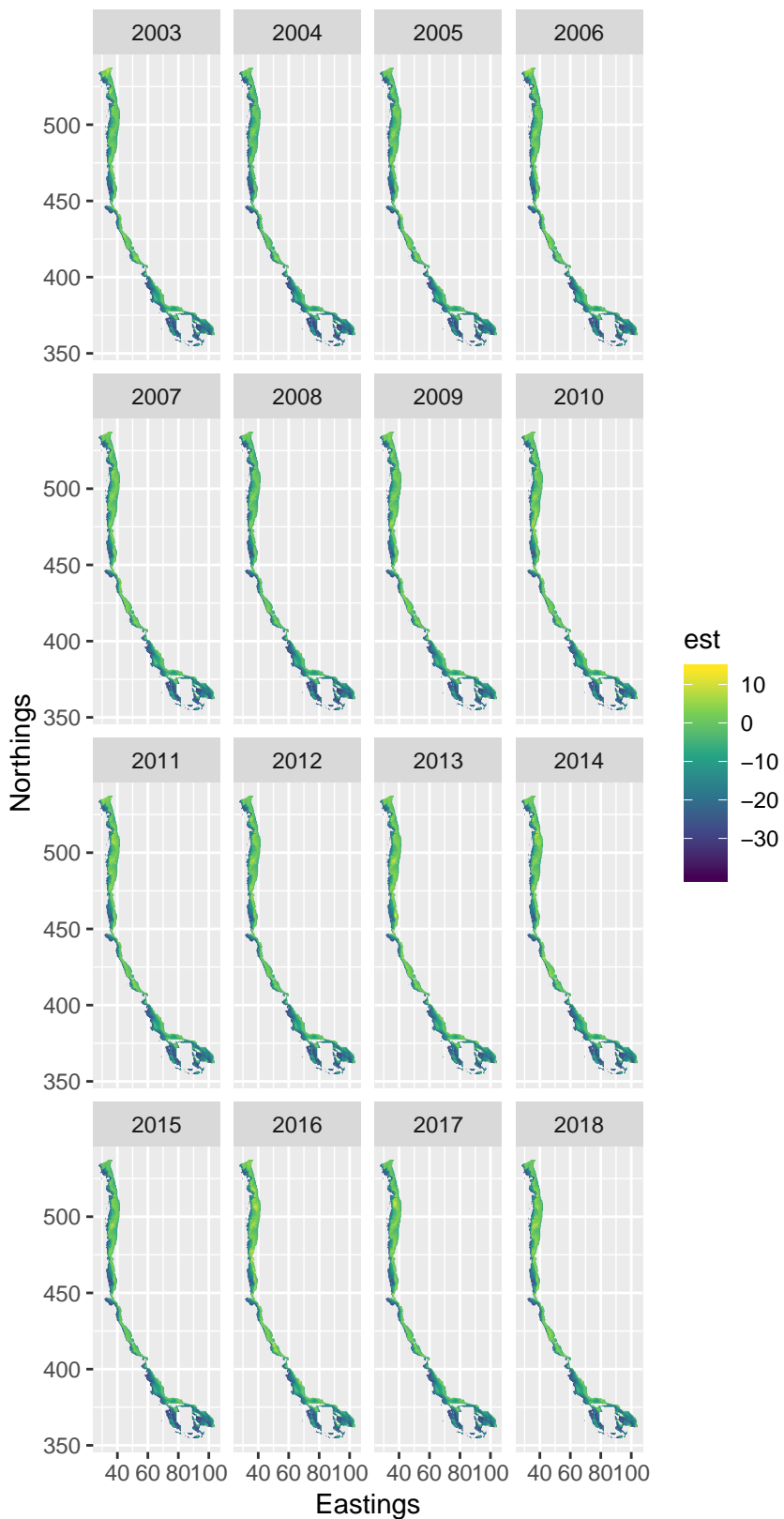


page 15 of 19  
Ecography  
shortspine thornyhead\_predicted\_density



page 17 of 19  
Ecography  
splitnose rockfish\_predicted\_density



page 19 of 19  
Ecography  
widow rockfish\_predicted\_density

**Recommendation by the Subject Editor (anonymous):**

This paper was read by two reviewers, both of whom saw value in the paper for the Ecography audience. However, both had concerns about the presentation and accessibility of the manuscript as currently written, which will take some hard work to address. A number of the statistical details need to be presented more clearly (and some potential statistical issues related to estimability and AIC addressed), and the overall framing presented more clearly to non-fisheries audiences. Ecography's readership works in a wide range of ecosystems, and this paper should be accessible to that range.

**Reviewer(s)' Comments to Author:**

Reviewer: 1

**Comments to the Author**

I was excited to read this manuscript as it presents a new way to detect shift in species distributions, which is clearly an important topic. Overall, I like the approach presented and think it will be a good contribution. I also think it fits well with Ecography's goals and scope. As you see below, however, I do have some reservations with the approach. In addition, I think many of the details are missing, which makes it hard to fully assess the validity of the method and the quality of the results.

**Major comments:**

1. In the methods section, most of the model details are lacking. I appreciate that part of the reason was potentially to keep the description general, but by doing so it makes it really hard for readers and reviewers to assess the validity of the method and nearly impossible to reproduce the method on their own data. Thus, I think the manuscript needs to present the full models (with all of the equations). I think it would make sense to present the full model for the fish data in details in the main text, thus including the observation equation, the link function, the distribution used for the random fields, the correlation structure (Mattern?), etc. I would also write down the full model for the simulation, but this could be placed in the supplementary material. I realize that the code is available, but this is not sufficient, the model must be described. Describing the model is essential to understand things like the parameters stated in Table S1 and the results presented in Fig. S1.

**We appreciate the desire of the reviewer and other readers to have these details readily available. We have revised the methods in the main text to include all relevant details and full equations. We have also added details regarding the simulations to the appendix as requested.**

2. I think these kinds of spatial random fields model suffer from Identifiability issues even without observation error and looking at the equation definitely make me fear that this is the case. The simulation studies should explore changes in the magnitude of all variance parameters ( $\sigma_0$ ,  $\sigma_{\{0, \text{trend}\}}$  in addition to  $\sigma_E$  and  $\phi$ ).

**There is an existing literature exploring these issues in models with the same essential structure, but without the spatial trend component. We modified the text to point the reader to these studies. Furthermore, to address the question in the context of this specific model, we performed additional simulations as recommended to determine how the magnitude of the spatial variance ( $\sigma_0$ ) and**

**spatial trend variance ( $\sigma_0$ \_trend) influence model performance. These results were in line with our intuition and are described in a new appendix figure (Fig. S2) along with additional text in the results of the main manuscript.**

3. I'm not a 100% sure what the theta is in the simulation results (e.g. in Fig 3). My understanding is that  $Z_s$  will have multiple values for a simulation (one for each point  $s$ ), so is theta the mean  $Z_s$  or are you taking each  $Z_s$  value of a simulation to be independent (then why not just call theta  $Z_s$  and  $\hat{Z}_s$ ?). I don't feel that either is great nor terrible, but knowing what it is definitely essential.

**What is shown in the figure are the distributions of location-by-location comparisons. We understand the confusion and have revised the text in the figure caption to clarify.**

4. My understanding is that AIC can be pretty poor at selecting between random effects due to parameter boundary problems. It would be worth using the simulation to see whether you can select between the model with and without the spatial trend. This could be done by fitting the model with and without the trends to your simulations and see whether you can recover the good model. You may need to add a model version without a spatial trend.

**We have now generated data with and without a spatial trend and compared models using AIC. We were able to recover the correct model and have summarized these results in a new figure (Fig. S3).**

5. Have you fitted the model with SST as a covariate and compared it with the trend model? It looks like some of the patterns are likely driven by changes temperature and it would help when understanding the patterns and support some of the statements in the discussion.

**We have not included such covariates because the purpose of the analysis was to provide the best description of the spatially-explicit temporal trends rather than ascribe them to specific dynamic environmental drivers. We would argue that this is out of scope and would need to be tackled in a separate paper. The purpose of the latent variable modeling approach here is to account for these unmodeled variables. We've already noted in the introduction and methods that other covariates could be included and cited literature where others have explored the costs and benefits of doing so. To further emphasize this, we have added text to the methods with additional citations and a sentence describing the reasoning for the latent variable approach described here.**

6. L217-225: it's only after reading the results and really digging into the figures that I understood what you are comparing. My understanding now is that what is done by others is calculate the COG either coastwise/for the whole range of species (which you call coarse-scale), or by sub-regions (which we could call med-scale?) - in your study there are 3 sub-regions divided by Point Conception and Cape Mendocino (you could specific these in a map and refer to it, see comment below for Fig 2). You are proposing that looking at the spatial trend ( $Z_s$ , which you call fine-scale) is much better. Could you please clarify this.

**We revised the final paragraph of the introduction to more explicitly set up the contrast from coarse-to fine-scale indicators, noting which approach applies to each and clarifying that this is a major**

**objective of the study.**

7. Similarly here, it took me a while to understand the clustering algorithm and its goal. I think it needs to be clarified here and likely needs its own paragraph (separated from the COG). I might be wrong, but my understanding is this is a non-spatial clustering technique that is used, and that the only spatial component is the latitude. Wouldn't you want to use a spatial clustering algorithm? Or something that allows to identify hotspots and coldspots? My intuition is that this would allow you to better identify the shifts inland that are discussed in the discussion. Here the cluster are really restricted by latitude and the patterns of the clusters are not particularly striking. I wonder (not sure if it makes sense), whether it would be worth plotting the change in COG for the clusters?

The reviewer is correct in thinking this is a nonspatial clustering technique, and we clarify this in the text. We do not use a spatial clustering technique because the spatial autocorrelation is already accounted for in the local trend model. Certainly, there are many ways that one could attempt to summarize the results of the local trend predictions more coarsely, and we have modified the text to acknowledge this point and emphasize that this is simply meant to serve as a qualitative summary of the spatial structure of the local trend. As for “hot” and “cold” spots, we already do this in Figure 4 by identifying which clusters had anomalously higher or lower values of the spatial trend. Regarding the influence of latitude on the cluster patterns, we experimented with clustering the local trend alone without latitude and the resulting patterns were quite similar if somewhat patchier in space. We have included this version as an appendix figure (Fig. S4). Finally, we also experimented with computing the COGs for each cluster rather than the biogeographic boundaries, and patterns were similar, yet we did not include the analysis in this form because we were concerned about potential confounding of the influence of latitude in the clustering and in weighting latitudes by density (as is done to compute the COG). In other words, we suspect that computing COGs by cluster would minimize and obscure distribution shifts, because if density is changing relatively uniformly over time within a cluster, one would expect the COG of that cluster to remain relatively constant. We have added an explanation of this reasoning into the relevant results section of the main text.

8. I don't find Fig 4 compelling. Almost none of the clusters matched the bottom line, and only a few matched the top line. What are you defining as near? I woonder if adding area boundaries to the second column of Fig 5 would better show your results? Or maybe the clusters are not really getting at these boundaries?

We modified the figure and caption, along with the supporting results text, to ease interpretation. Specifically, we added a buffer around each line depicting the biogeographic boundaries, which we use to formally assess whether a break (the maximum or minimum latitude of a local trend cluster) is proximal to one of these boundaries. We added text to the results providing statistics on the proportion of species for which cluster breaks fell within these buffer areas, or between these two areas yet outside the buffer zone. We also added lines depicting the regions defined by these biogeographic barriers to the first panel of column 2 in Figure 5 as suggested.

Minor comments:

The title is not really selling the paper. It feels like you are comparing metrics that are already available, but in fact you are proposing a new method.

**We revised the title to better represent the main objective of the paper and hint at the novelty of the method. We refrain from declaring that we are using a new model or new method because the degree to which a change in approach represents a “novel method” is subjective, and we want to avoid being overly grandiose. However, we now refer to this as a “new approach” in the abstract.**

L147: I think it's a bad idea to call it spatial trend. You are trying to get a temporal trend? I think generally spatial trend is understood to be a systematic (and generally smooth) change in the mean value of a variable over an area. Here it's just a random field no (and from Fig 5 it not particularly smooth and systematic)? And the main interest is that it demonstrates how the other random field change through time.

**To avoid confusion, we define this additional random slope field as the spatially explicit temporal trend, but have introduced a new term to replace “spatial trend” as the shorthand for this term, by replacing this phrase with “local trend” throughout.**

L153: I realize that the model presented is likely a state-space model, especially when we include the observation error, but nowhere is it referred as such (and actually the observation equation is never presented), so this connection is not clear. Worth mentioning above that it is a state-space model. Also, would it be a state-space if there were no observation error?

**There is no explicit observation model. However, even without an observation model, it is still a state space model because the random effects are estimated at the knot locations and predicted to the data locations. However, we do not think there is a benefit to describing the model using state-space model terminology as it could also be labeled as a mixed effects model (as we describe it in the text) or random effects model and using state-space terminology may confuse the matter for some readers.**

L170-182: Could you add 1-2 sentences describing the survey effort.

**We added additional details regarding the survey methods and data, as requested.**

I would number all of the equations. It helps to refer to them.

**Added equation numbers as requested.**

Fig. 2 Please add boundaries around the 3 sub-regions and/or large lines at the two breaks, so the sub-regions are clear.

**We did not include lines separating these boundaries in this figure because at this point in the main text, there has not been a reference to these subregions. However, we do include labels for the locations that serve as latitudinal boundaries separating the region and clearly explain this in the figure legend. Furthermore, we added reference lines to Figure 4 that correspond to these**

**boundaries.**

Fig 3. why is sigma=1 (which according to table S1 was explored) is not presented?

This is a really really small detail, but it would help quickly understand the results (without going back to the table S1), if you had 0.01 rather than 0.00 on the y-axis.

**We have clarified which levels of the parameters were evaluated in the figure caption to address both of these comments. We did not show the results for sigma=1 because they differed little from sigma=0.75, thus we simplified the figure to focus on the main gradients/thresholds. We added text to the figure caption describing this reasoning.**

Fig.5 Why the mean density value over all years? Why not the value at t 0 and final time, to show the trends. Even if it's not striking, it might make the point that just comparing the predicted value at time 0 and last year is less powerful than looking at the trend estimated. The map projection is also strange.

**We chose the mean density over all years because this can be interpreted as the “weight” on the local trend, serving as a basis for discussing how distributions change relative to their average distribution. We consider this a more important point for explaining distribution shifts than simply pointing out that the trend is more interesting than a comparison of distributions at the initial and final time (a point which was already made more rigorously by comparing post-hoc regression to estimate local trends rather than estimating the trend within the model). We added text to the methods to describe this reasoning explicitly. As for the map projection, we agree that it is slightly distorted but prefer this projection as it makes the prediction surfaces easier to see, rather than being extremely laterally compressed.**

Reviewer: 2

#### Comments to the Author

Thank you for giving me the opportunity to review the manuscript “Comparing metrics of species distribution change across spatial scales with spatiotemporal models”. The authors present a new modeling approach to account for spatial and temporal variability in species density and distribution. I find the title somewhat misleading as I don’t see this as a comparison but rather the introduction of a new model. Although I am familiar with species distribution models, I’m afraid I found the paper hard to follow and some of the figures completely indecipherable. I fear the utility of the paper may be lost on someone unfamiliar with fisheries.

**We revised the title to highlight our development of a novel approach. We also performed a major reorganization and revision of the introduction to broaden the scope and further emphasize relevance to fields beyond fisheries. The same modeling approach can be applied to many other forms of biological and environmental data. We have also revised the figures, figure captions, and methods to clarify the main points they are meant to communicate.**

As a terrestrial species biologist I found myself looking for terrestrial analogies and trying to understand the methods in that context. The authors cite Yackulic et al 2013 who provide a review of MAXENT and

presence only data. I wonder if a better comparison would be to the extensive literature on spatially explicit mark recapture (SECR) that easily incorporates temporal and spatial variation in species density. I'm obviously biased and perhaps this is an unfair criticism but I wonder if the paper could be made more broadly approachable by adding comparisons to spatial mark recapture and or terrestrial systems and surveys?

**We added additional text and citations to the introduction and discussion to provide more direct analogies to established terrestrial approaches to species distribution modeling and multiple data types.**

If I understand correctly a major limitation in the model is that it requires a linear trend in density and distribution. Given the introduction I assumed that the model would take into account species density rather than distribution to better track population trend (i.e. a shift in distribution may suggest a decline in population that is not supported if density is accounted for). I'm left wondering what happens if a decline is not systematic and why this is better (as stated on line 170).

**We are unclear on what the referee is asking here, but it seems to arise from some slight misunderstandings. Indeed, the model does predict population density at each location and does not make any strict assumptions about the temporal trend in abundance of the whole population. To rectify similar potential misunderstandings, we have worked to improve clarity throughout, including a more explicit explanation of what is meant by references to a linear response. To clarify, a linear model in this context is one where the response is a linear function of the coefficients. However, this does not mean that all response variables must have a linear relationship with covariates. We also note that if nonlinear responses in many local areas are present in the data, one could adapt the model to account for this (now noted at end of first methods section).**

Lines 34-37 – You provide examples of the ranges of things that might be have distributions we want to track, but you don't anything about what might cause distribution shifts. Might also be beneficial to add a sentence regarding what causes distribution shifts.

**We added some text in this first paragraph of the introduction to clarify the mechanisms by which distributions change.**

Line 40 – “However, when reliable population density data are available, distribution shifts are better quantified by spatial predictions of population size” This statement might benefit from the support of a citation.

**While there is not necessarily a great citation that demonstrates this directly, it can be understood to be true based on first principles. We modified the text to make the link between these sentences and subsequent paragraph stronger, where we have references that demonstrate how the hypothesis that the distribution of abundance within a species range is greatest at the center and declines smoothly toward the range edge (the abundant-center hypothesis) has been debunked (Sagarin and Gaines 2002, Sagarin et al. 2006). We also added additional text to this first paragraph of the introduction to explain why population size data is inherently richer than say, presence/absence data.**

Line 55 – I found this transition a little distracting. I don't find the choice of appropriate scale any more or less germane to this question than any other in ecology so am not sure this is necessary.

**We added a citation (Connor et al. 2019) to better emphasize why scale is a particularly important issue in SDMs.**

Line 109 – This is the first use of SDM in the manuscript so the acronym needs to be defined.

**Defined SDM as species distribution model upon this first use, as requested.**

Line 149 – Figure 1, like all of the figures in the manuscript excluding figure 2, is a bit of a challenge. Judging from the model is it necessary that the trend be linear from year to year? I'm not sure what it is the authors are trying to convey here in the figure.

**To clarify the message, we added another axis label to the figure to indicate that the numbers represent time steps. In addition, we added more text to the figure caption and methods to better explain the main point. With regard to the question about linear assumptions, please see our response to the referee's general comments. Additional information regarding this approach has already been published in (Anderson and Ward 2019).**

Figure 4 – I find it almost impossible to decipher anything from this figure.

**We modified the figure and caption, along with the supporting results text, to ease interpretation.**

Figure 5 – labeling the North American continent may make it more readily apparent that each tile represents the west coast. What do the colors in column 2 represent? There is no legend.

**The study region was established in figure 2, so we'd hope that the reader would recall this. However, to clarify we added a label identifying the land area as the US west coast and a reminder of the study location in the figure caption. We did not include a legend for colors in column 2 because they simply represent different clusters of the spatial trend (as labeled at the top of this column), and since species differ in their number of clusters, a single legend would be inadequate or confusing. However, to clarify this we now include a more explicit description of what these colors represent in the figure caption.**

**Literature Cited in Response**

- Anderson, S. C., and E. J. Ward. 2019. Black Swans in Space: Modeling Spatiotemporal Processes with Extremes. *Ecology* 100:e02403.
- Connor, T., A. Viña, J. A. Winkler, V. Hull, Y. Tang, A. Shortridge, H. Yang, Z. Zhao, F. Wang, J. Zhang, Z. Zhang, C. Zhou, W. Bai, and J. Liu. 2019. Interactive spatial scale effects on species distribution modeling: The case of the giant panda. *Scientific Reports* 9:14563.
- Sagarin, R. D., and S. D. Gaines. 2002. The ‘abundant centre’ distribution: to what extent is it a biogeographical rule? *Ecology Letters* 5:137–147.
- Sagarin, R. D., S. D. Gaines, and B. Gaylord. 2006. Moving beyond assumptions to understand abundance distributions across the ranges of species. *Trends in Ecology & Evolution* 21:524–530.